Spring 1995

Closed-Loop Identification of Unstable Systems in Time and Frequency Domains

Hyun Chang Lee
Old Dominion University

CLOSED-LOOP IDENTIFICATION OF UNSTABLE SYSTEMS IN TIME AND FREQUENCY DOMAINS

by

Hyun Chang Lee

B.S. February 1981, Inha University, Korea
M.S. February 1983, Inha University, Korea
M.S. May 1989, Univ. of Maryland, College Park, MD., USA

A Dissertation Submitted to the Faculty of Old Dominion University
in partial fulfillment of the requirements for the degree of

Doctor of Philosophy
Engineering Mechanics

Old Dominion University
May, 1995

Approved by:

_____
Dr. Jen-Kuang Huang (Director)

_____
Dr. Colin Britcher

_____
Dr. Sebastian Bawab

_____
Dr. Gene Hou

ABSTRACT

CLOSED-LOOP IDENTIFICATION OF UNSTABLE SYSTEMS IN TIME AND FREQUENCY DOMAINS

Hyun Chang Lee
Old Dominion University, 1995
Director: Dr. Jen-Kuang Huang

This dissertation presents closed-loop identification algorithms of an unstable system in the time and frequency domains. In the time domain, the projection filter, which is a linear transformation which projects (transforms) a finite number of input-output data of a system into its current space, is used to relate the state-space model with a finite difference model. The method developed can take into account the effects of process noise as well as measurement noise and identify open-loop systems with unknown feedback dynamics in the closed-loop operation. Then the recursive relations between Markov parameters and the ARX model are derived to identify recursively the system, controller and Kalman filter Markov parameters, which are finally used to identify the system, controller and Kalman filter gains. The closed-loop test data demonstrate that the open-loop state-space model identified by using projection filters is fairly accurate in predicting the step responses while the analytical model has several deficiencies. In the frequency domain, the relation between

the closed-loop system matrices and the frequency response function is derived to identify system parameters. Also a simulation model of uncertainty to design a robust controller is proposed by using the maximum singular value of unstructured uncertainties caused by underestimated modes and noise. The uncertainty model developed here can be tested and used for the design of a high-performance robust controller in the future. The NASA Large-Angle Magnetic Suspension Test Facility (LAMSTF) is used to validate the algorithms developed.

ACKNOWLEDGEMENT

The bliss and satisfaction, that comes with the successful completion of any task couldn't be complete until the expression to the people who made it possible. I would like to acknowledge my debt to all those who have somehow contributed to my knowledge and inspiration.

I would like to thank my advisor, Dr. Jen-Kuang Huang, from whom I have received attentive instruction, care and guidance. The members of my doctoral committee, Dr. Colin Britcher, Dr. Gene Hou and Dr. Sebastian Bawab are greatly appreciated for their constructive suggestions in revising the dissertation. I also want to express my sincere thanks to Dr. M.-H. Hsiao who gave me a lot of guide at the beginning of my study at Old Dominion University. Also thanks to Mr. David Cox, research engineer at NASA Langley Research Center, who provided the test data for the NASA LAMSTF system.

The dissertation will not be possible without my parent's and parent-in-law's support and encouragement. Special thanks go to my wife, Kim, Sooknyeo, and our daughters, Christina (Geeyeon) Lee and Helena (Seyeon) Lee for their patience, love and sacrifice. I want to cherish the memory of my former advisor, Dr. Kim, Sang-Cheol, who inspired me to start graduate study and passed away in Korea last December.

CONTENTS

LIST OF TABLES

LIST OF FIGURES

ABBREVIATIONS

ARX	AutoRegressive with eXogeneous input
CLID	Closed-Loop Identification
ERA	Eigensystem Realization Algorithm
ERA/DC	Eigensystem Realization Algorithm/ Data Correlations
FFT	Fast Fourier Transformation
FRF	Frequency Response Function
IDFT	Inverse Discrete Fourier Transform
LQG	Linear Quadratic Gaussian
LQR	Linear Quadratic Regulator
LAMSTF	Large-Angle Magnetic Suspension Test Facility
NASA	National Aeronautics and Space Administration
OKID	Observer/Kalman Filter Identification
OCID	Observer/Controller Identification
SSFD	State-Space Frequency Domain
SVD	Singular Value Decomposition

LIST OF SYMBOLS

A, B, C	open-loop system matrices
A_c, B_c, C_c	closed-loop system matrices
A_d, B_d, C_d, D_d	system matrices of dynamic controller
a_i, b_i, c_i, d_i	coefficient matrices of ARX model
D	damping matrix
F	state feedback gain
F_q	projection filter
G	control influence matrix
H	Hankel matrix
I	identity matrix
i, j, k	integer number
K	Kalman filter gain
l	data length
M	mass matrix
m	number of outputs
N	open-loop Kalman filter Markov parameter
N_c	closed-loop Kalman filter Markov parameter
n	number of states
$P_{x\xi}$	covariance between x_k and ξ_k
Q	weighting matrix for system state in performance index
q	order of ARX model

R	weighting matrix for system input in performance index
R_ξ	auto-covariance of ξ_k
r	reference input
s	Laplace transformation or number of inputs
u	control input
u_f	feedback input
V	covariance matrix of measurement noise
v	measurement noise
W	covariance matrix of process noise
w	process noise
x	system state
Y	open-loop system Markov parameter
Y_c	closed-loop system Markov parameter
Y_d	controller Markov parameter
y	system output
Z	output data and feedback input data matrix
z	z-transform
$\| \|_2$	2-norm
∞	infinity

Greek Letters

α_i, β_i	coefficient matrices of transfer function matrix
ε	residual after filtering
ϕ	input-output data matrix
η	augmented state of open-loop system and controller
θ	augmented coefficient matrix of ARX model
ξ	overall noise vector

Subscripts and Superscripts

k	k-th time step
T	matrix transpose
-1	matrix inverse

Notations above a Symbol

^	estimate
-	expected value

Chapter 1

INTRODUCTION

1.1 Background and Problem Statement

System identification is the process of developing or improving a mathematical model of a physical system based on its input-output data. Achieving high control performance on these systems usually requires an accurate model. Such a model can be derived from system identification techniques using experimental data. The more engineers understand about system properties through system identification, the better system control design and performance can be achieved. The mission of the system identification community is to provide effective and accurate analytical tools which include the understanding methodologies, computational procedures and their implementation. The development of good analytical tools demand a mathematical understanding of the problem to be solved and an appreciation for the numerical precision required when handling a large amount of data. System identification is very important in active control of aerospace structures as well as many other fields such as robotics, civil engineering structures, electrical circuits, etc.

Basically, the procedure involves four key steps of system modeling, system identification testing, controller design and verification tests. In the structural field, the finite element technique is used almost exclusively for constructing analytical models in the form of second-order differential equations. This approach is well-established and normally provides a model sufficient for structural design analysis. However, it is known from experience that the finite element model without refinement through dynamic tests is not accurate enough for use in designing a vibration control system for structures. Once the structure is built, static and dynamic tests are performed to construct a mathematical model that characterizes the dynamics of the system at the selected control and measurement positions. The mathematical model is then used for controller designs that complete the feedback loop for active control of the flexible system. The final step is to verify the closed-loop performance by conducting closed-loop dynamic tests.

The major benefit of system identification is the improvement of the analytical model of a structure. Quite often, the initial numerical (e.g., finite element) model of a structure is found to be incorrect by as much as 10% in the lowest frequencies. These inaccuracies are due to a combination of factors, including, but not restricted to: approximations in the finite element derivations; mismodeling of structural elements; differences in actual material properties and dimensions from those assumed in the model; and lack of convergence of the numerical model. Since the mid-sixties, the field of system identification has been an important discipline within the automatic control area. One reason is the requirement that mathematical models having a specified accuracy must be used to apply modern control methods. Another reason is technological developments in several areas, i.e., high quality integrated sensors and actuators, powerful control processors that can implement complex control algorithms, and powerful computer hardware and software that can be used to design and analyze control systems.

Frequency- and time-domain methods give complementary views of many important problems in linear system theory and control theory. Sometimes, the two methods have been viewed as rivals, particularly on issues of implementation and application to real systems. Historically, frequency-domain methods dominated theory and practice of system identification in control engineering prior to the 1960s whereas the time-domain approach has dominated the control engineering literature on system identification over the past twenty years. However, not all investigators agreed on the advantages of time-domain approach over frequency-domain approach, and a significant minority led by H. H. Rosenbrock and A. J. G. MacFarlane remain unconvinced to the present day. The complaint of the frequency-domain advocates is that the reason for the use of the feedback is the uncertainties in the dynamic process, and that when these uncertainties are present, the qualitative methods of frequency-domain analysis are more appropriate. Qualitative system properties such as bandwidth, stability margin, etc., were regarded as difficult to study by state-space methods.

Recently, a method has been developed to compute the Markov parameters of a linear system, which are the same as its pulse response history[1-8]. The method, referred to as the Observer/Kalman Filter Identification algorithm (OKID) is formulated entirely in the time domain, and is capable of handling general response data. By introducing an observer to identification equations, this method makes it possible to identify not only the open-loop system, but also an associated observer which can be later used in controller design. Depending on the noise characteristics, the method identifies a deadbeat observer which is the fastest possible observer in the absence of noise, or a Kalman filter which is an optimal observer in the presence of noise, or any other observer with user specified poles. The approach based on an observer can use a much smaller order of AutoRegressive with eXogeneous (ARX) input model than one derived through a Kalman filter, but the derivation is based on a deterministic approach. For a stochastic system and an ARX model of a small

order, to what the least-squares identification of the ARX model will converge in a stochastic sense is not clear. In order to solve this problem, projection filters, which were originally derived for deterministic systems[9], are developed for identification of linear stochastic systems[6,10].

An important extension of the above OKID method is the identification of closed-loop systems. For identifying marginally stable or unstable systems, feedback control is required to ensure overall system stability. These methods still can be applied by using the bounded open-loop input-output data obtained during closed-loop operation. However, it is generally harder to identify the open-loop system from open-loop input-output data because it is difficult to ensure that the input signal to the plant has sufficient frequency richness to excite all of the system's dynamics. For an unstable system, the input-output data are not even available while it is under an open-loop operation. To use those methods directly, we have to design a controller and input signal to the closed-loop system so that the input signal to the open-loop system is almost white. Unfortunately, this is very difficult, if not impossible.

To overcome the problems described, Closed-Loop IDentification algorithms (CLID)[11-14] have been proposed for identifying a system under closed-loop operation. However, the proposed CLID have several shortcomings. First, the Kalman filter can't be simultaneously identified because the proposed methods are applied only for a deterministic systems. In Reference 13, no recursive form was derived for computing the open-loop system Markov parameters. In Reference 14, the approach is based on the system pulse response. Generally speaking, random excitation provides better result of identification than pulse input because the noise from random excitation response can be removed through a least squares method. For the case where the existing controller dynamics are assumed to be unknown, a method

was developed in Reference 11, referred as the Observer/Controller Identification algorithm (OCID), to identify an open-loop model, and an effective observer/controller combination.

It has been found that the OKID and CLID methods can effectively identify the state-space models using time domain input-output data. However, there are cases in which frequency response data, rather than time histories, are available. This is the often case with the advent of sophisticated spectrum analyzers and associated automatic test equipment. Many researchers also found that LQG control, which was the dominant player in the birth of modern control, optimality and design of optimal control system, failed to work in real environments. In a series of papers, researchers showed that LQG-based designs could become unstable in practice as more realism was added to the plant model.[15] It became apparent that too much emphasis on optimality, and not enough attention to the model uncertainty issue, was the main culprit. Therefore, the technique of obtaining state-space models from frequency response data is of practical interest to active control applications.

Recently, a method called the State-Space Frequency Domain (SSFD) identification algorithm has been developed for open-loop system.[16] In Reference 16, the method uses a rational matrix function to curve-fit frequency data and obtains the Markov parameters from this equation. In obtaining the state-space models from the Markov parameters, the Eigensystem Realization Algorithm (ERA),[17] or its variant ERA/DC,[18] is used. The disadvantage of this method is that curve-fitting problem must either be solved by non-linear optimization techniques or by linear approximate algorithms requiring several iterations.[16] In Reference 19, the method uses a matrix-fraction for the curve-fitting for a open-loop system and the curve-fitting is reformulated as a linear problem which can be solved by the ordinary least-squares method in one step. The other hand, most of recent work in this area have been concentrated on the robust control issue. Even though a variety of approaches to this problem were investigated by many researchers, many questions are still remained to be

answered. The researches in the area have been well documented in the special issue on system identification for robust control design of the IEEE Transactions on Automatic Control.[20]

1.2 Objective

The objective of this dissertation is to develop an effective closed-loop system identification algorithm in the time and frequency domains to overcome some of the problems associated with existing identification methods.

In time domain, the projection filter, which is a linear transformation which projects (transforms) a finite number of input-output data of a system into its current space, is used to relate a space-space model with a finite difference model. The method developed in this dissertation can take into account the effects of process noise as well as measurement noise in closed-loop operation. Then recursive relation between Markov parameters and the ARX model are derived to identify recursively the system, controller and Kalman filter Markov parameters which are finally used to identify system matrices and controller Kalman filter gains.

In frequency domain, the relation between the closed-loop system matrices and Frequency Response Function (FRF) is derived to identify system parameter and Kalman filter gains. From this relationship, the method to obtain state-space models from frequency response data is derived. Also, when there is no enough information or confidence about suitable number of state modes, which has been one of the main reason for the unstructured uncertainty, it will be shown how the underestimated state number affect results to cause

uncertainty in identification. A simulation model of uncertainty is proposed to use the underestimated state modes and the process and measurement noises.

1.3 Dissertation Outline

Chapter 2 provides background material about existing closed-loop identification methods. Th recursive relations for closed-loop system and Kalman filter Markov parameters are derived through z-transform, and the relation between closed-loop and open-loop Markov parameters are summarized. A constant-gain full-state feedback controller case is also reviewed.

Chapter 3 provides the description of the NASA's Large-Angle Magnetic Suspension Test Facility (LAMSTF). The system matrices are also provided and used for numerical simulations in the following chapters. The analytical model shows that the system is highly unstable. Because it is difficult to accurately model the magnetic field and its gradients, the analytical model contains some modeling error.

Chapter 4 presents a derivation of the closed-loop identification for a stochastic system to include processing and measurement noise through a projection filter. After a short review of closed-loop identification is given, the relation between the Kalman filter and projection filter is explained. The recursive relation is investigated to obtain Markov parameters for the system, Kalman filter and controller from the coefficients of ARX model with projection filter. Simulation and test results from LAMSTF are followed to validate the proposed algorithm.

Chapter 5 presents derivation of the relation between system matrices and Frequency Response Function (FRF) for the stochastic system operating in the closed-loop system. After the relation between state-space and FRF is reviewed for open-loop system, the same is derived for closed-loop case. A discussion of uncertainty is followed by numerical examples.

Chapter 6 provides conclusions and prospects for the extension of this research.

Chapter 2

EXISTING CLOSED-LOOP IDENTIFICATION

2.1 Introduction

In this chapter, the derivation of closed-loop identification is summarized. The underlying concept within control theory that has made it into a field of science is feedback. The study of feedback and its properties is responsible for the rapid growth of this field. There are two important properties that a feedback system possesses that an open-loop system cannot have. These are reduced sensitivity and disturbance rejection. By reduced sensitivity it is meant that feedback reduces the sensitivity of the closed-loop system to uncertainties or variations in elements located in the forward path of the system. Disturbance rejection refers to the fact that feedback can eliminate or reduce the effects of unwanted disturbances occurring within the feedback loop. An open-loop system can also eliminate certain disturbances (an input is generated that subtracts off the measurable disturbances), but it requires full knowledge of disturbance, which is not always available.

Most existing system identification methods[21-23] apply for stable systems without requiring feedback control for identification purpose. For identifying marginally stable or unstable systems, feedback control is required to ensure overall system stability. These methods still can be applied by using the bounded open-loop input-output data obtained during closed-loop operation. however, it is generally harder to identify the open-loop system from open-loop input-output data because it is difficult to ensure that the input signal to the plant has sufficient frequency richness to excite all of the system's dynamics. The method summarized in the following section was presented to identify a linear open-loop stochastic system from closed-loop input-output data in time domain without recording feedback signals.[24] The method can be applied to some other cases when a system, although stable, is operated in closed-loop and it is impossible to remove the existing feedback controller for open-loop identification. Additionally, whether the system is stable or not, the feedback controller can be used as a design parameter for system identification. One may choose a controller to enhance the damping and thus reduce the closed-loop input-output data required for identification.

Closed-loop identification can simultaneously identify the open-loop state-space model of a system and the corresponding Kalman filter when the system is under closed-loop operation. The first step in the process is deriving the relation between the closed-loop state-space model and AutoRegressive with eXogeneous (ARX) input models for stochastic systems. From the derivation, it can be seen that a state-space model can be represented by an ARX model if the order of the ARX model is chosen large enough. Since the relation between the input-output data and the system parameters of an ARX model is linear, a linear programming approach like least-square methods can be used for the ARX model parameter estimation. Second, the algorithm to compute the open-loop system and Kalman filter Markov parameters from the estimated ARX model parameters is derived. In this step, the closed-loop system and Kalman filter Markov parameters from the estimated ARX model

parameters is computed, and then the open-loop system and Kalman filter Markov parameters from the closed-loop ones are computed. Third, the state-space model for the open-loop system is realized from the open-loop Markov parameters through the singular value decomposition method.[17,25] Finally, the Kalman filter for the open-loop system can be estimated from the realized state-space model and the open-loop Kalman filter Markov parameters through the least-squares approach.

2.2 Closed-Loop State-Space Model and ARX Model

A finite-dimensional, linear, discrete-time, time-invariant system can be modeled as:

$$x_{k+1} = Ax_k + Bu_k + w_k \tag{2.1}$$

$$y_k = Cx_k + v_k . \tag{2.2}$$

where $x \in R^{n\times 1}$, $u \in R^{s\times 1}$, $y \in R^{m\times 1}$ are state, input and output vectors, respectively; w_k is the process noise, v_k the measurement noise; $[A,\ B,\ C]$ are the state-space parameters. Sequences w_k and v_k are assumed Gaussian, white, zero-mean, and stationary with covariance matrices Q and R respectively. One can derive a steady-state filter innovation model[26]:

$$\hat{x}_{k+1} = A\hat{x}_k + Bu_k + AK\varepsilon_k \tag{2.3}$$

$$y_k = C\hat{x}_k + \varepsilon_k . \tag{2.4}$$

where $\hat{x}_k$ is the a priori estimated state, K is the steady-state Kalman filter gain and ε_k is the residual after filtering: $\varepsilon_k = y_k - C\hat{x}_k$. The existence of K is guaranteed if the system is detectable and $(A, Q^{1/2})$ is stabilizable[27].

On the other hand, any kind of dynamic output feedback controller can be modeled as:

$$p_{k+1} = A_d p_k + B_d y_k \tag{2.5}$$

$$u_k = C_d p_k + D_d y_k + r_k, \tag{2.6}$$

where A_d, B_d, C_d, and D_d are the system matrices of the dynamic output feedback controller, p_k the controller state and r_k the reference input to the closed-loop system. Combining (2.3) to (2.6), the augmented closed-loop system dynamics becomes

$$\eta_{k+1} = A_c \eta_k + B_c r_k + A_c K_c \varepsilon_k \tag{2.7}$$

$$y_k = C_c \eta_k + \varepsilon_k, \tag{2.8}$$

where

$$\eta_k = \begin{bmatrix} \hat{x}_k \\ p_k \end{bmatrix}, A_c = \begin{bmatrix} A + BD_d C & BC_d \\ B_d C & A_d \end{bmatrix}, B_c = \begin{bmatrix} B \\ 0 \end{bmatrix},$$

$$A_c K_c = \begin{bmatrix} AK + BD_d \\ B_d \end{bmatrix}, \text{and } C_c = [C \quad 0]. \tag{2.9}$$

It is noted that K_c can be considered as the Kalman filter gain for the closed-loop system and the existence of the steady-state K_c is guaranteed when the closed-loop system matrix A_c is nonsingular.

$$y_k = \sum_{i=1}^{\infty} C_c \bar{A}^{i-1} A_c K_c y_{k-i} + \sum_{i=1}^{\infty} C_c \bar{A}^{i-1} B_c r_{k-i} + \varepsilon_k. \tag{2.10}$$

where $\bar{A} = A_c - A_c K_c C_c$ and is guaranteed to be asymptotically stable because the steady-state Kalman filter gain K_c exists. Since $\bar{A}$ is asymptotically stable, $\bar{A}^i \approx 0$ if $i > q$ for a sufficiently large number q (discussed in Ref. 10). Thus (2.10) becomes

$$y_k \approx \sum_{i=1}^{q} a_i y_{k-i} + \sum_{i=1}^{q} b_i r_{k-i} + \varepsilon_k \tag{2.11}$$

where

$$a_i = C_c \bar{A}^{i-1} A_c K_c, \; b_i = C_c \bar{A}^{i-1} B_c. \tag{2.12}$$

The model described by (2.11) is the ARX model which directly represents the relationship between the input and output of the closed-loop system. The coefficient matrices a_i and b_i can be estimated through least-squares methods from a random excitation input r_k and the corresponding output y_k. From (2.11) it can be seen that parameters of the ARX model are linearly related to the closed-loop input-output data. Therefore, solving for an ARX model involves solving a linear programming problem involving an over-determined set of equations.

2.3 Markov Parameters

In the previous section, an ARX model, which represents a closed-loop system, is identified from the closed-loop input/output data through the least-squares method. With known controller dynamics, the estimated ARX model can be transformed to an open-loop state-space model by the following steps. First, the closed-loop system and Kalman filter Markov parameters are calculated from the estimated coefficient matrices of the ARX model. Second, the open-loop system and Kalman filter Markov parameters are derived from the closed-loop system Markov parameters, the closed-loop Kalman filter Markov parameters, and the known controller Markov parameters. Third, the open-loop state-space model is realized by using singular-value decomposition for a Hankel matrix formed by the open-loop system Markov parameters. Finally, an open-loop Kalman filter gain is calculated from the realized state-space model and the open-loop Kalman filter Markov parameters through least-squares.

The z-transform of the open-loop state-space model (2.3) yields

$$\hat{x}(z) = (z - A)^{-1}(Bu(z) + AK\varepsilon(z)). \tag{2.13}$$

Substituting (2.13) to the z-transform of (2.4), one has

$$y(z) = C(z-A)^{-1}(Bu(z) + AK\varepsilon(z)) + \varepsilon(z)$$

$$= \sum_{k=1}^{\infty} Y(k)z^{-k}u(z) + \sum_{k=0}^{\infty} N(k)z^{-k}\varepsilon(z), \tag{2.14}$$

where $Y(k) = CA^{k-1}B$ is the open-loop system Markov parameter, $N(k) = CA^{k-1}AK$ open-loop Kalman filter Markov parameter, and $N(0) = I$ which is an identity matrix. Similarly, for the dynamic output feedback controller (2.5) and (2.6) and the closed-loop state-space model (2.7) and (2.8), one can derive

$$u(z) = \sum_{k=0}^{\infty} Y_d(k)z^{-k}y(z) + r(z) \tag{2.15}$$

$$y(z) = \sum_{k=1}^{\infty} Y_c(k)z^{-k}r(z) + \sum_{k=0}^{\infty} N_c(k)z^{-k}\varepsilon(z), \tag{2.16}$$

where $Y_d(k) = C_d A_d^{k-1} B_d$ is the controller Markov parameter, $Y_c(k) = C_c A_c^{k-1} B_c$ the closed-loop system Markov parameter, and $N_c(k) = C_c A_c^{k-1} A_c K_c$ the closed-loop Kalman filter Markov parameters. It is also noted that $Y_d(0) = D_d$ and $N_c(0) = I$.

The z-transform of the ARX model (2.11) yields

$$\left(I - \sum_{i=1}^{q} a_i z^{-i}\right) y(z) = \sum_{i=1}^{q} b_i z^{-i} r(z) + \varepsilon(z). \tag{2.17}$$

Applying long division to (2.17), one has

$$y(z) = [b_1 z^{-1} + (b_2 + a_1 b_1)z^{-2} + (b_3 + a_1(b_2 + a_1 b_1) + a_2 b_1)z^{-3} + \ldots]r(z)$$
$$+ [I + a_1 z^{-1} + (a_1 a_1 + a_2)z^{-2} + (a_1(a_1 a_1 + a_2) + a_2 a_1 + a_3)z^{-3} + \ldots]\varepsilon(z).$$

After comparing with (2.16), the closed-loop system and Kalman filter Markov parameters can be recursively calculated from the estimated coefficient matrices of the ARX model,

$$Y_c(k) = b_k + \sum_{i=1}^{k} a_i Y_c(k-i) \tag{2.18}$$

$$N_c(k) = \sum_{i=1}^{k} a_i N_c(k-i). \tag{2.19}$$

It is noted that $Y_c(0) = 0$, $N_c(0) = I$, and $a_i = b_i = 0$, when $i > q$. One may obtain (2.18) and (2.19) from (2.12) and the definition of the Markov parameters[3,4]. However, the derivation is much more complex.

Next, the open-loop system and Kalman filter Markov parameters can be derived from the closed-loop system Markov parameters, the closed-loop Kalman filter Markov parameters, and the known controller Markov parameters. Substituting (2.15) into (2.14) yields

$$\begin{aligned} y(z) &= \left(\sum_{k=1}^{\infty} Y(k) z^{-k}\right)\left(\sum_{k=0}^{\infty} Y_d(k) z^{-k} y(z)\right) + \sum_{k=1}^{\infty} Y(k) z^{-k} r(z) + \sum_{k=0}^{\infty} N(k) z^{-k} \varepsilon(z) \\ &= \sum_{k=1}^{\infty} \alpha_k z^{-k} y(z) + \sum_{k=1}^{\infty} Y(k) z^{-k} r(z) + \sum_{k=0}^{\infty} N(k) z^{-k} \varepsilon(z), \end{aligned} \tag{2.20}$$

where $\alpha_k = \sum_{i=1}^{k} Y(i) Y_d(k-i)$. Rearranging (2.20), one has

$$\left(I - \sum_{k=1}^{\infty} \alpha_k z^{-k}\right) y(z) = \sum_{k=1}^{\infty} Y(k) z^{-k} r(z) + \sum_{k=0}^{\infty} N(k) z^{-k} \varepsilon(z). \tag{2.21}$$

Similarly, one can apply long division to (2.21), and then compare it with (2.16), to describe the closed-loop system Markov parameters recursively in terms of the open-loop system and the controller Markov parameters,

$$Y_c(j) = Y(j) + \sum_{k=1}^{j} \alpha_k Y_c(j-k) = Y(j) + \sum_{k=1}^{j} \sum_{i=1}^{k} Y(i) Y_d(k-i) Y_c(j-k). \tag{2.22}$$

And the closed-loop Kalman filter Markov parameters can be recursively expressed in terms of the open-loop system Markov parameters, the open-loop Kalman filter Markov parameters, and the controller Markov parameters,

$$N_c(j) = N(j) + \sum_{k=1}^{j} \alpha_k N_c(j-k) = N(j) + \sum_{k=1}^{j} \sum_{i=1}^{k} Y(i) Y_d(k-i) N_c(j-k). \qquad (2.23)$$

Rearranging (2.22) and (2.23), one has

$$Y(j) = Y_c(j) - \sum_{k=1}^{j} \sum_{i=1}^{k} Y(i) Y_d(k-i) Y_c(j-k) \qquad (2.24)$$

$$N(j) = N_c(j) - \sum_{k=1}^{j} \sum_{i=1}^{k} Y(i) Y_d(k-i) N_c(j-k). \qquad (2.25)$$

Equations (2.24) and (2.25) show that one can recursively calculate the open-loop system and Kalman filter Markov parameters from the closed-loop system Markov parameters (from (2.18)), the closed-loop Kalman filter Markov parameters (from (2.19)), and the known controller Markov parameters $Y_d(k) = C_d A_d^{k-1} B_d$. It is noted that $Y_c(0) = 0$ and $N_c(0) = I$. One can easily verify (2.24) and (2.25) from (2.9), and also from the definition of the Markov parameters.

2.4 State-Space Realization

The open-loop state-space model can be realized from the open-loop system Markov parameters through the Singular Value Decomposition (SVD) method[17,25]. The first step is to form a Hankel matrix from the open-loop system Markov parameters,

$$H(j) = \begin{bmatrix} Y(j) & Y(j+1) & \cdots & Y(j+\beta) \\ Y(j+1) & Y(j+2) & \cdots & Y(j+\beta+1) \\ \vdots & \vdots & \ddots & \vdots \\ Y(j+\gamma) & Y(j+\gamma+1) & \cdots & Y(j+\gamma+\beta) \end{bmatrix}, \qquad (2.26)$$

where $Y(j)$ is the j-th Markov parameter. From the measurement Hankel matrix, the realization uses the SVD of $H(1)$, $H(1)=U\Sigma V^T$, to identify a n-th order discrete state-space model as

$$A=\Sigma_n^{-1/2}U_n^T H(2)V_n\Sigma_n^{-1/2},\ B=\Sigma_n^{1/2}V_n^T E_s,\ C=E_m^T U_n\Sigma_n^{1/2}, \tag{2.27}$$

where matrix Σ_n is the upper left hand $n\times n$ partition of Σ containing the n largest singular values along the diagonal. Matrices U_n and V_n are obtained from U and V by retaining only the n columns of singular vectors associated with the n singular values. Matrix E_m is a matrix of appropriate dimension having m columns, all zero except that the top $m\times m$ partition is an identity matrix. E_s is defined similarly.

2.5 Identification with Full-State Feedback

In this section, the above closed-loop identification problem is considered for a particular case. If a constant-gain full-state feedback controller is used, the open-loop system can be identified by following a simpler procedure.[24] An open-loop system with a full-state sensor and a constant gain full-state feedback controller can be modeled as:

$$x_{k+1}=Ax_k+Bu_k+w_k \tag{2.28}$$

$$y_k=x_k+v_k \tag{2.29}$$

$$u_k=-Fy_k+r_k, \tag{2.30}$$

where F is the known constant feedback gain and r_k is the reference input to the closed-loop system. After applying filter innovation model[26] to the open-loop system and eliminating control input u_k, the closed-loop system becomes

$$\hat{x}_{k+1}=(A-BF)\hat{x}_k+Br_k+(AK-BF)\varepsilon_k \tag{2.31}$$

$$y_k = \hat{x}_k + \varepsilon_k. \tag{2.32}$$

Comparing (2.31) and (2.32) with (2.7) and (2.8), one can have $\eta_k = \hat{x}_k$, $A_c = A - BF$, $B_c = B$, $A_c K_c = AK - BF$, and $C_c = I$. Then one can identify the *closed-loop* system matrices and Kalman filter gain by the same way as the proceeding section. If the *identified* closed-loop system matrices and Kalman filter gain are described by a quadruplet, $[\hat{A}_c, \hat{B}_c, \hat{C}_c, \hat{A}_c\hat{K}_c]$, one needs to transform it to the same coordinate used in (2.31) and (2.32), so that the controller dynamics can be removed from the closed-loop system. Since full-state feedback is used, the identified output matrix $\hat{C}_c$ is a square matrix, and is generally invertable. Then one may use $\hat{C}_c^{-1}$ as the transformation matrix to transform the identified quadruplet to be $[\hat{C}_c\hat{A}_c\hat{C}_c^{-1}, \hat{C}_c\hat{B}_c, I, \hat{C}_c\hat{A}_c\hat{K}_c]$ where I is an identity matrix. Comparing the transformed quadruplet with (2.31) and (2.32), on can easily obtain

$$A - BF = \hat{C}_c\hat{A}_c\hat{C}_c^{-1},\ B = \hat{C}_c\hat{B}_c,\ AK - BF = \hat{C}_c\hat{A}_c\hat{K}_c. \tag{2.33}$$

The identified open-loop system matrices and Kalman filter gain become

$$A = \hat{C}_c\hat{A}_c\hat{C}_c^{-1} + \hat{C}_c\hat{B}_c F,\ B = \hat{C}_c\hat{B}_c,\ C = I,\ K = A^{-1}(\hat{C}_c\hat{A}_c\hat{K}_c + BF). \tag{2.34}$$

If sensors are available to provide all the state information, one can choose a constant-gain controller (e.g. a pole-placement controller or a Linear Quadratic Regulator (LQR)) so that the closed-loop system has the same dimension as the open-loop system. This controller can be designed (e.g. by adjusting the weighting matrices in the LQR controller) so that the closed-loop system is very easy to identify. For example, a closed-loop system with poles located within a desired frequency range with similar damping ratios between 0.4 to 0.7 may be easily identified.

2.4 Coordinate Transformation

For any dynamic system, although its system Markov parameter is unique, the realized state-space model is not unique. If one needs to compare the identified state-space model with the analytical model, both models have to be in the same coordinates. In this section, a unique transformation matrix is derived to transform any realized state-space model to a form usually used for a structural dynamic system so that any identified system parameter can be compared with the corresponding analytical one.[28] This unique transformation matrix exists only when one half of the states can be measured directly. If this condition is not satisfied, other transformation matrices may exist but they are usually not unique.

Consider a structural dynamic system

$$M\ddot{p} + D\dot{p} + Kp = Gu \tag{2.35}$$

where p is displacement, u control force, G control influence matrix and M, D and K are mass, damping and stiffness matrices, respectively. Then the state-space equation and output equation are,

$$\dot{x} = A_m x + B_m u \text{ and } y = C_m x, \tag{2.36}$$

where $x = \begin{Bmatrix} p \\ \dot{p} \end{Bmatrix}$, $A_m = \begin{bmatrix} 0 & I \\ -M^{-1}K & -M^{-1}D \end{bmatrix}$, $B_m = \begin{bmatrix} 0 \\ M^{-1}G \end{bmatrix}$ and C_m is the output matrix. If half of the states can be measured directly, then $C_m = [I \quad 0]$. Now, one may first convert the realized discrete-time system $[A,B,C]$ to a continuous-time system $[A_c,B_c,C]$. If A is diagonalized by matrix Q, then

$$Q^{-1}AQ = \Lambda \tag{2.37}$$

$$A_c = Q\frac{\ln(\Lambda)}{T}Q^{-1} \tag{2.38}$$

$$B_c = (A - I)^{-1} A_c B \tag{2.39}$$

where T is sampling time. It is assumed that the matrix $\begin{bmatrix} C \\ CA_c \end{bmatrix}$ is full rank. Let the transformation matrix

$$P = [P_1 \quad P_2] = \begin{bmatrix} C \\ CA_c \end{bmatrix}^{-1}, \tag{2.40}$$

then

$$P^{-1}P = \begin{bmatrix} C \\ CA_c \end{bmatrix} [P_1 \quad P_2] = \begin{bmatrix} CP_1 & CP_2 \\ CA_cP_1 & CA_cP_2 \end{bmatrix} = \begin{bmatrix} I & 0 \\ 0 & I \end{bmatrix} \tag{2.41}$$

$$P^{-1}A_cP = \begin{bmatrix} C \\ CA_c \end{bmatrix} A_c [P_1 \quad P_2] = \begin{bmatrix} CA_cP_1 & CA_cP_2 \\ CA_c^2P_1 & CA_c^2P_2 \end{bmatrix} = \begin{bmatrix} 0 & I \\ X & X \end{bmatrix} \tag{2.42}$$

$$CP = [CP_1 \quad CP_2] = [I \quad 0]. \tag{2.43}$$

Note that $CP = C_m$. As a result, the identified continuous-time model $[A_c, B_c, C]$ can be transformed to be $[P^{-1}A_cP, P^{-1}B_c, CP]$ which is in the form of Eq. (2.36). Then both the identified and analytical models are in the same coordinate and can be compared.

Chapter 3

NASA LAMSTF CONFIGURATION

3.1 Introduction

In this chapter, the Large Angle Magnetic Suspension Test Facility (LAMSTF) is introduced and used as the example for the closed-loop identification. This facility has been assembled at NASA Langley Research Center for a ground-based experiment that can be used to investigate the technology issues associated with magnetic suspension at large gaps, accurate suspended-element control at large gaps, and accurate position sensing at large gaps. This technology is applicable to future efforts that range from magnetic suspension of wind tunnel models to advanced spacecraft experiment isolation and pointing systems.[28]

This facility basically consists of five electromagnets (see Figure 3.1) which actively suspend a small cylindrical permanent magnet. The cylinder is a rigid body and has six independent degrees of freedom, namely, three displacements (x, y and z) and three rotations (pitch, yaw and roll). The roll of the cylinder is uncontrollable and is assumed to be motionless. Five pairs of LEDs and photo-detectors are used to indirectly sense the pitch

and yaw angles, and three displacements of the cylinder's centroid. The inputs consist of five currents into five electromagnets and the outputs are five voltage (position) signals from five photo-detectors. Very briefly, the currents into the electromagnets generate a magnetic field which produces a net force and torque on the suspended cylinder.

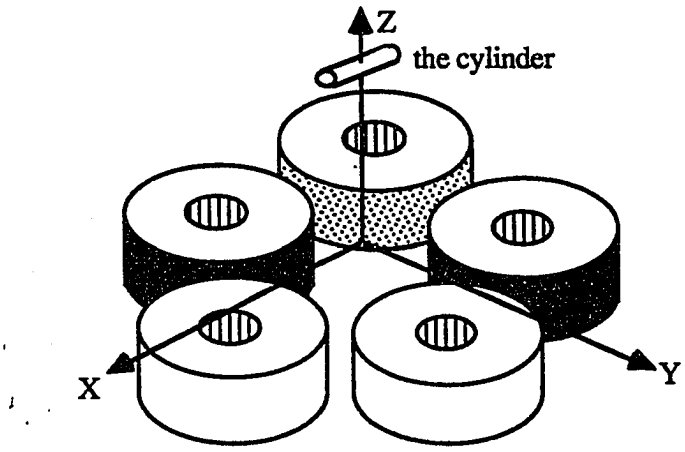

Figure 3.1 Large-Angle Magnetic Suspension Test Facility (LAMSTF) configuration.

The details of the suspended cylinder, the coils, power amplifiers, and the position sensors are described in the following sections.[29] The mathematical model of this system has been derived in detail in references 30 and 31. Only the final system matrices will be provided in the later section.

3.2 Suspended Cylinder

The suspended cylinder is an aluminum tube filled with 16 wafers of Neodymium-Iron-Boron permanent magnet material. The aluminum tube is about 5.32 cm long and 0.525 cm outside diameter. The wafers are arranged in N-S-N-S sequence and are epoxied. Each magnetic wafer is 0.7963 cm in diameter and 0.3135 cm long. The suspended cylinder is levitated at a height of about 10 cm above the coils.

3.3 Coils and Power Amplifiers

There are five coils mounted on the perimeter of a circles of about 13.77 cm radius, at a spacing of 72° apart, an a 1/2" thick, square aluminum plate. The coils are made of 509 turns of AWG 10 enameled copper wire wound on bakelite spools, with soft iron cores. The windings on the coils are covered with epoxy resin to reduce deformity due to high current forces. The currents through the coils are controlled by five switching power amplifiers, capable of delivering a maximum of 30A continuous and 60A peak. The amplifiers have a switching frequency of 22kHz, and require a DC. supply of 150V. The amplifiers function in a voltage-to-current converter mode and are set in a gain of 3 A/V to have a flat response. The coils can't adequately dissipate the thermal energy generated in them due to their internal resistance. To protect against thermal runaway, each coil has been equipped with a temperature sensing device, which is monitored by a set of five digital temperature controllers. The temperature controllers are set to disable the power amplifiers at 160° F.

3.4 Position Sensors

The detection of the suspended cylinder's position is performed by five sets of infrared LEDs and photo-detectors. These LED-photo-detector pairs are installed in two perpendicular planes (vertical and horizontal), which allow detection of five degrees-of-freedom of the cylinder (see Figure 3.2). The beams from the infrared LEDs, which are incident on the photo-detectors, would be partially blocked by the cylinder. The relative position of the cylinder can then be determined from the amount of light received by the photo detectors. This method is common in wind tunnel magnetic suspension applications and has been quite successful. From Figure 3.2, pairs 1 and 3 are used to detect the pitch angular and z linear displacements. Pitch 2 is used to detect the x displacement. Pairs 4 and

5 are used to detect the yaw angular and y linear displacements. The range of the sensors is founded to be about ± 1° for pitch and yaw and ±0.5 mm for x, y, and z axes.

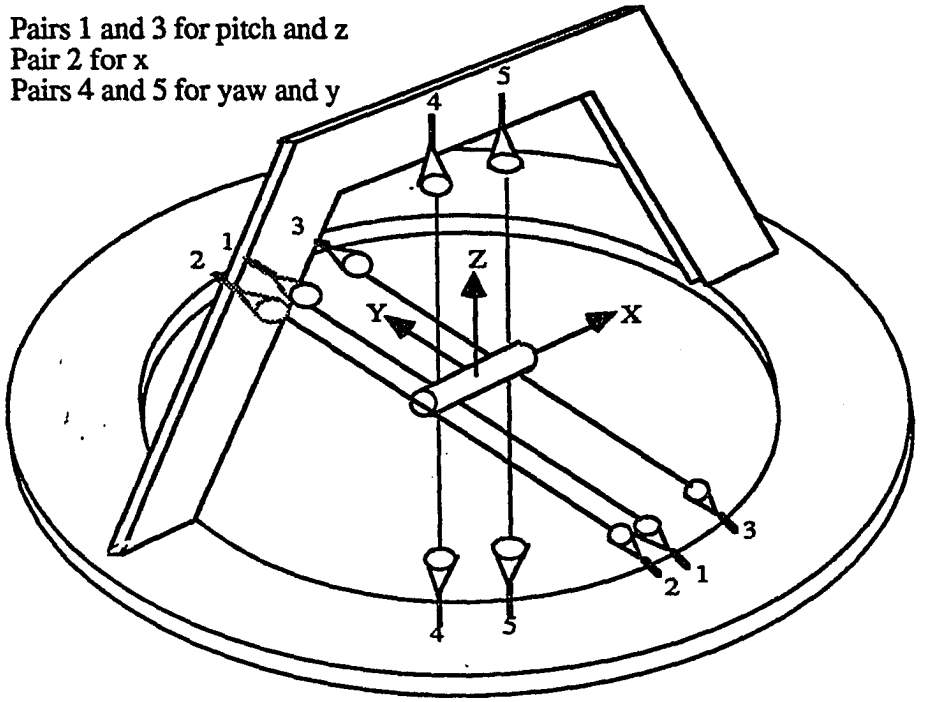

Figure 3.2 Position sensors of the cylinder

3.5 System Modeling

The analytical model of this system has been derived in detail in References 30 and 31. This model can be obtained by combining two equations. One is the equation of motion for the cylinder dynamics. The other is the equation which relates the magnetic force and torque on the cylinder generated by the currents of the coils. Both equations are non-linear. After linearizing both equations and excluding the bias inputs for overcoming the gravity of the cylinder, one can have the state-space model

$$\dot{x} = A_m x + B_m u \tag{3.1}$$

$$y = C_m x \tag{3.2}$$

where $x = \begin{Bmatrix} x_p \\ \dot{x}_p \end{Bmatrix}$, $A_m = \begin{bmatrix} 0_{5\times5} & I_{5\times5} \\ A_{21} & A_{22} \end{bmatrix}$, $B_m = \begin{bmatrix} 0_{5\times5} \\ B_2 \end{bmatrix}$ and $C_m = [C_1 \quad 0_{5\times5}]$. The state variable x_p includes pitch and yaw angles and three linear displacements of the cylinder's centroid. The matrices A_{21}, A_{22}, B_2 and C_1 are

$$A_{21} = \begin{bmatrix} 3341.5 & 0 & -39392 & 0.0000 & 0.0000 \\ 0 & 3341.5 & -0.0000 & 0.0000 & -0.0000 \\ -9.8070 & -0.0000 & 49.937 & 0.0000 & -0.0251 \\ -0.0000 & 0 & 0.0000 & 95.577 & -0.0000 \\ -0.0000 & -0.0000 & -0.0251 & -0.0000 & -0.9132 \end{bmatrix},$$

$$A_{22} = 0_{5\times5},$$

$$B_2 = \begin{bmatrix} 38.370 & 38.370 & 38.370 & 38.370 & 38.370 \\ 0 & 89.802 & 55.514 & -55.514 & -89.802 \\ 0.2214 & -0.1527 & 0.0784 & 0.0784 & -0.1527 \\ 0 & 0.1215 & -0.1967 & 0.1967 & -0.1215 \\ -0.2767 & -0.0854 & 0.2238 & 0.2238 & -0.0854 \end{bmatrix}.$$

$$C_1 = \begin{bmatrix} 89.024 & 0 & 0 & 0 & 6097.6 \\ 0 & 0 & 7874.0 & 0 & 0 \\ -116.25 & 0 & 0 & 0 & 6250.0 \\ 0 & 95.425 & 0 & -6535.9 & 0 \\ 0 & -107.25 & 0 & -5181.3 & 0 \end{bmatrix}.$$

The eigenvalues of the system matrix A_m are listed in Table 3.1. The corresponding mode shapes are shown in Figure 3.3. As shown, three modes are unstable, and the other two are marginally stable. The matrix C_1 which relates the sensor output voltage to the displacement can be obtained from calibration and is assumed to be deterministic. To recover the displacement from the sensor output voltage, one can use $x_p = C_1^{-1} y$.

3.6 Concluding Remarks

The NASA LAMSTF configuration has been described. The analytical model has been derived in detail in References 30 and 31. From open-loop eigenvalues, it has been found that there are three unstable modes and two stable oscillatory modes. Because it is difficult to accurately model the magnetic field and its gradients, the analytical model contains some modeling errors. Since the system is unstable, the bounded input-output data can be obtained only from closed-loop operation. Closed-loop identification is thus required to validate this model and is presented in the proceeding chapter. The process noise may include temperature effects on the coils, inevitable electrical noise, and error of the bias inputs used to overcome the weight of the cylinder. The measurement noise is caused by the non-linearity and saturation of the sensors and inevitable electrical noise.

Table 3.1 Open-loop modes of the suspended cylinder

Mode #	Eigenvalues	Stability	Degree of Freedom
1	±58.78	unstable	x, θ_y (axial, pitch)
2	±j7.97	stable oscillatory	x, θ_y (axial, pitch)
3	±57.81	unstable	θ_z (yaw)
4	±j0.96	stable oscillatory	z (vertical)
5	±9.78	unstable	y (lateral)

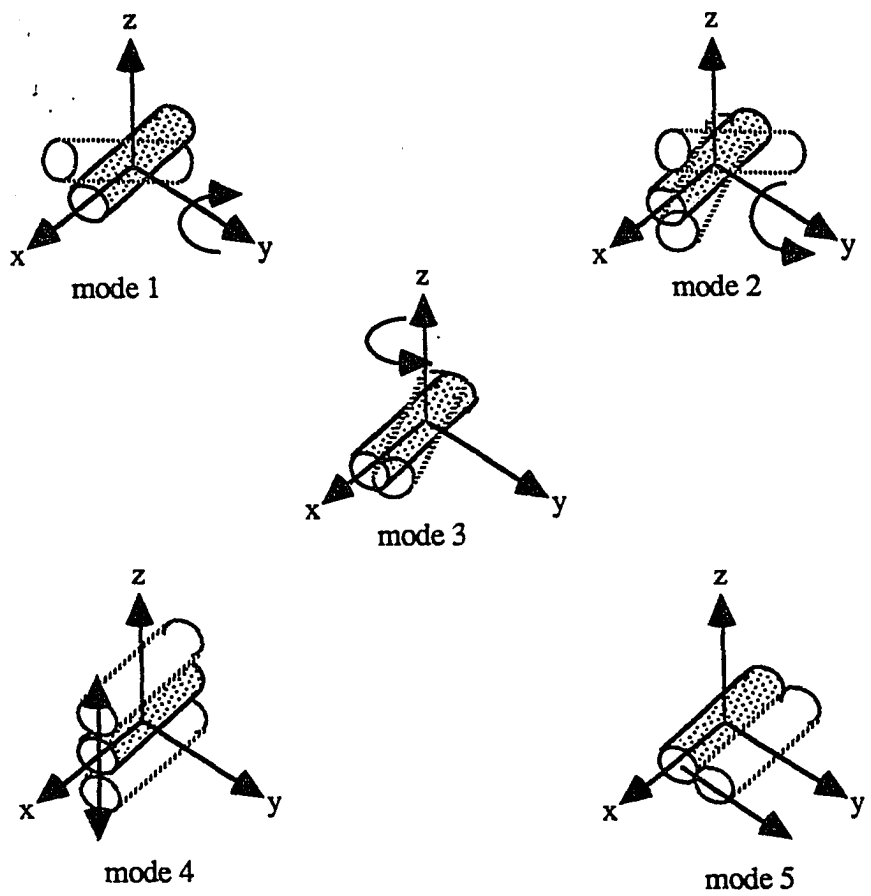

Figure 3.3 Mode shapes of LAMSTF configuration from analytical model

Chapter 4

CLOSED-LOOP IDENTIFICATION WITH UNKNOWN FEEDBACK DYNAMICS

4.1 Introduction

Recently, methods have been developed to compute the Markov parameters of a linear system from the open-loop input-output data.[1,4,10] By including an observer or Kalman filter in the state-space equation, both the open-loop plant and an associated observer or Kalman filter can be identified and used for further controller design. Further progress was made for identifying an open-loop system, observer, and controller from closed-loop test data.[11] There are several instances when such a need arises. For example, the system may be operating in closed-loop with an existing feedback controller and only closed-loop data are available for identification. This is particularly true for identifying unstable systems. However, the method derived in Ref. 11 is based on a *deterministic* approach. The effect of the process and measurement noise was not considered. To handle the noise effect, Kalman filters have been widely used.

The great body of literature reveals the importance of the Kalman filter; however, at the same time it reveals the existence of some unsatisfactory features as well. A well-known limitation in applying the conventional Kalman filter is its requirement of a priori knowledge about the system state-space model and the covariances of process and measurement noises. This information, in practice, is either only partially known or totally unknown. Another limitation of the conventional Kalman filter is that it can neither adjust itself to trace a changing environment, nor can it correct the error caused by incorrect a priori information. In a sense, the conventional Kalman filter works as an open-loop system, because the filter evolves according to present formulas during operations and the estimation error never affects the filter itself. Moreover, after reaching its steady state, the filter "sleeps". That is, no matter how big the estimation error could be due to whatever reasons, the filter just remains unchanged. A phenomenon called filter divergence could happen.[32-35] On the other hand, projection filters are developed to identify stochastic systems from open-loop input-output data.[6] The approach is primarily based on the relationship between the state-space model and the AutoRegressive with eXogeneous input (ARX) model, via the projection filter. This paper extends the above development to the identification of an open-loop stochastic system operating in closed-loop with or without feedback dynamics.

Figure 4.1 shows a schematic diagram of an actual closed-loop stochastic system with existing feedback controller. The open-loop system dynamics, Kalman filter gain and controller are assumed to be unknown. The closed-loop system is excited by a known excitation signal, and the closed-loop system response and the feedback signal are measured. It is noted that for modeling a stochastic system, the Kalman filter gain K has to be included in the system dynamics A,B,C and D matrices. The Kalman filter gain represents the input matrix for the noises in the innovation model.[26] A schematic diagram of the identified closed-loop system is shown in Fig. 4.2, where $\hat{A},\hat{B},\hat{C},\hat{D}$ represent the

identified open-loop system matrices, $\hat{K}$ and $\hat{F}$ represent the identified Kalman filter and controller gains, respectively.

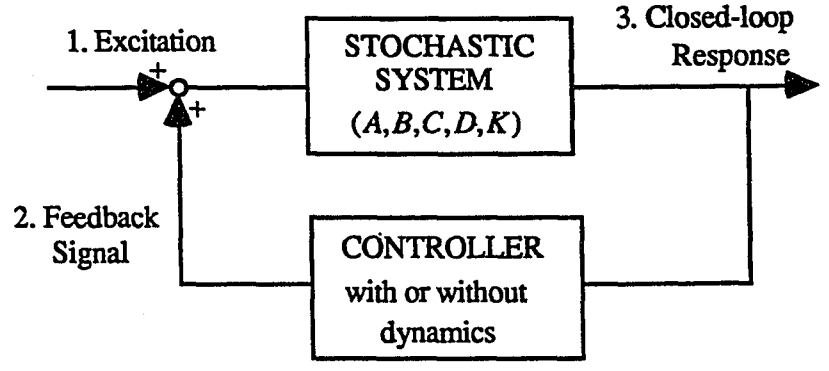

Fig. 4.1 Actual stochastic system with existing controller.

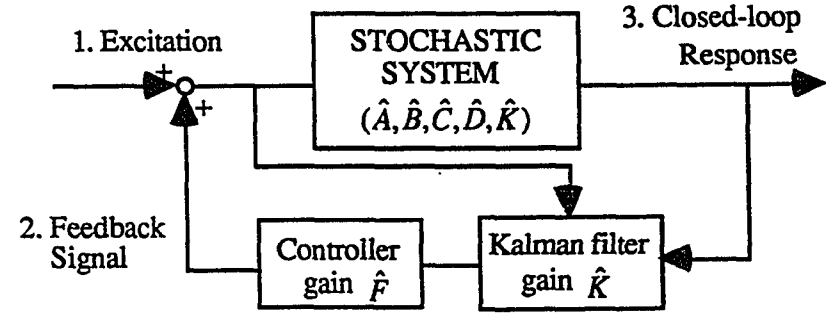

Fig. 4.2 Identified stochastic system with effective controller.

In this chapter, the relation between Kalman and Projection filters is discussed in the second section. Then identification algorithm with projection filter is presented in the third section followed by numerical examples and experimental results. To identify the model with projection filter, the projection filter is first derived from the relationship between the state-space model and the ARX model including the system, Kalman filter and controller. The ARX model is chosen and the ordinary least-squares method is used to estimate the coefficient matrices from the closed-loop control input, system response and feedback

signal. Markov parameters of the open-loop system, Kalman filter and controller gains are then calculated from the coefficients of the identified ARX models. Finally, the state-space model of the open-loop stochastic system and the gain matrices for both Kalman filter and controller are realized through the Eigensystem Realization Algorithm (ERA).[17] The method is validated in the last section by numerical example and experimental results from the unstable Large-Angle Magnetic Suspension Test Facility described in chapter 3.

4.2 Relationship between Kalman and Projection Filter

As discussed at chapter 2.2, (2.3) and (2.4) are the best description of a stochastic system, whose state-space model is shown in (2.1) and (2.2) in a Kalman filter sense. The model using the presentation of (2.3) and (2.4) is called a filter innovation model. This model will be used in the derivation of the closed-loop identification.

The projection filter is a linear transformation which projects (transforms) a finite number of input-output data of a system into its current state-space. The filter is designed such that the mean square estimation error is minimized; therefore, the image of the projection is an optimal estimate of the current state. In other words, by defining a measurement vector $Y_{q,k}$ as

$$Y_{q,k} = \begin{bmatrix} y_k \\ y_{k-1} \\ \vdots \\ y_{k-q+1} \end{bmatrix}, \tag{4.1}$$

the projection filter is the matrix F_q such that

$$\hat{x}_k = F_q Y_{q,k}, \tag{4.2}$$

which provides an optimal estimate $\hat{x}_k$ of the current state x_k. In the above equations q denotes the number of successive previous measurements, including the current one, contained in the measurement vector. The transformation matrix F_q is called the *projection filter* of order q. Here the generic term "filter" is used to represent the data processing procedure which receives measurement as input and produces the information interested as output. The projection filter and the Kalman filter are closely related. In fact, a projection filter of order q $(q \geq 2)$ can be transformed to have a Kalman filter structure, and the recursive projection filter of order one is identical to the Kalman filter. The identity of the two filters can be proved by re-deriving the Kalman filter through the recursive projection filter of order one. Mathematical derivation of the relationship has already been well documented in the references.[36] Here only a brief conceptual explanation will be given.

The a priori values of the estimates q and their corresponding error covariances of the projection filter are either obtained by propagating from their initial values or by setting them to be the steady state values. However, the counterparts in the Kalman filter are conditional means and covariances, conditioned on all previous data. Using conditional means as the a priori estimates allows the Kalman filter to utilize all the data (from the beginning till the current moment) recursively in estimating the current state. On the contrary, a projection filter of order q uses only q most recent data to do the same task. As a result, the Kalman filter in general is more accurate than a projection filter of small order. Besides, the Kalman filter treats only one measurement at each step, while the projection filter of order q needs to treat a batch of q data. Therefore, computationally the Kalman filter is more efficient.

One might ask if the projection filter can somehow be modified to have the capability of utilizing all the data available so that it may produce the same result as the Kalman filter. The answer is yes. Because both filters are optimal linear filters, based on the same given

conditions, they should be equivalent. For a projection filter with order of q, a number of q's most recent measurements should be kept in record at each step. The estimate made at each step does not take advantage of previous estimates. In other words, the estimation is totally based on the finite data in the current record. In order to use all measurements, one may increase the order as the time step increases, However, by doing that, the computational load will soon become too heavy to bear in practice. Hence, from a computational point of view, a recursive type of projection filter is preferable.

For recursive projection filters of orders greater than one in which the recursive feature is obtained by using conditional a priori mean and state covariance, the formulations are the same as the Kalman filter. In this case, some measurements are used more than once in estimating one single state, that is, some measurements are used both in calculating the a priori estimate and in calculating the filter part, or the modifying part. However, this does not help in improving the results. Since the projection filter seeks the conditional mean of the state, it makes no difference whether a measurement is conditioned once, twice, or more. Consequently, a recursive projection filter of an order greater than one is computationally inefficient. Though there is no benefit in computation, the concept of the projection filter is still valuable. The property of equivalence between the recursive projection filter and the Kalman filter helps in the development of an effective system identification method.

4.3 Identification with Projection Filter

4.3.1 Relationship between Projection Filter and ARX Model

To explain the relationship between the projection filter and the ARX model of a linear stochastic system, consider a finite-dimensional, linear, discrete, time-invariant stochastic dynamic system represented by a state-space model as

$$x_{k+1} = Ax_k + Bu_k + w_k \tag{4.3}$$

$$y_k = Cx_k + Du_k + v_k \tag{4.4}$$

where $x_k \in R^{n\times 1}$ is the state vector, $u_k \in R^{m\times 1}$ the input vector, $y_k \in R^{p\times 1}$ the measurement or output vector , $w_k \in R^{n\times 1}$ the process noise, and $v_k \in R^{p\times 1}$ the measurement noise. The noises w_k and v_k are assumed to be white, Gaussian with zero mean and uncorrelated. Matrices A,B,C, and D are the state matrix, input matrix, output matrix and direct transmission matrix respectively. The integer k is the sample indicator.

In Fig. 4.1, the control input u_k to the plant is the summation of the random excitation signal r_k and the feedback signal $u_{f,k}$. The existing controller can be a full state feedback controller or any dynamic controller. Assuming for the moment, the existing controller is a full state feedback controller with a gain F,

$$u_k = r_k + u_{f,k} \tag{4.5}$$

$$u_{f,k} = -Fx_k. \tag{4.6}$$

From Eqs. (4.3) and (4.4), it is easy to show that

$$\begin{bmatrix} y_k \\ y_{k-1} \\ y_{k-2} \\ \vdots \\ y_{k-q+1} \end{bmatrix} = \begin{bmatrix} C \\ CA^{-1} \\ CA^{-2} \\ \vdots \\ CA^{-q+1} \end{bmatrix} x_k - \begin{bmatrix} -D & 0 & \cdots & \cdots & 0 \\ 0 & CA^{-1}B-D & \cdots & \cdots & 0 \\ \vdots & CA^{-2}B & CA^{-1}B-D & \cdots & \vdots \\ \vdots & \vdots & \vdots & \ddots & \vdots \\ 0 & CA^{-q+1}B & \cdots & \cdots & CA^{-1}B-D \end{bmatrix} \begin{bmatrix} u_k \\ u_{k-1} \\ u_{k-2} \\ \vdots \\ u_{k-q+1} \end{bmatrix}$$

$$- \begin{bmatrix} 0 & \cdots & \cdots & \cdots & 0 \\ CA^{-1} & \cdots & \cdots & \cdots & 0 \\ \vdots & \ddots & \ddots & \ddots & \vdots \\ \vdots & \ddots & \ddots & \ddots & \vdots \\ CA^{-q+1} & \cdots & \cdots & \cdots & CA^{-1} \end{bmatrix} \begin{bmatrix} w_k \\ w_{k-1} \\ \vdots \\ \vdots \\ w_{k-q+1} \end{bmatrix} + \begin{bmatrix} v_k \\ v_{k-1} \\ \vdots \\ \vdots \\ v_{k-q+1} \end{bmatrix}, \tag{4.7}$$

or in short

$$Y_{q,k} = H_q x_k - G_q U_k - M_q W_{q,k} + V_{q,k}, \tag{4.8}$$

or in a normal form

$$H_q x_q = Y'_{q,k} + \xi_{q,k}, \tag{4.9}$$

where $Y'_{q,k} = Y_{q,k} + G_q U_k$ and $\xi_{q,k} = M_q W_{q,k} - V_{q,k}$. Note that the unknown x_k is a random variable in this case. Now the overall noise vector $\xi_{q,k}$ is still Gaussian and zero-mean because $W_{q,k}$ and $V_{q,k}$ are Gaussian and zero-mean, but it is correlated with x_k because $W_{q,k}$ is correlated with x_k. Now denote the covariance between x_k and $\xi_{q,k}$ by $P_{x\xi}$ and the auto-covariance of $\xi_{q,k}$ by R_ξ. For (4.13), given the mean of the current state $\bar{x}_k$ and its variance P_x, by the theory of random parameters estimation[37] the optimal estimate of x_k can be obtained by

$$\hat{x}_k = \bar{x}_k + F_q(Y'_{q,k} - \bar{Y}'_{q,k}) \tag{4.10}$$

where the overbar "-" denotes the expected value,

$$\bar{Y}'_{q,k} = H_q \bar{x}_k \tag{4.11}$$

and

$$F_q = (P_x H_q^T + P_{x\xi})(H_q P_x H_q^T + H_q P_{x\xi} + P_{x\xi}^T H_q^T + R_\xi)^{-1}. \tag{4.12}$$

The matrix F_q is the projection filter. The optimality is defined by minimum variance of state estimator error. To derive an ARX model, one can form an one-step-ahead output prediction using the estimated state of the last step, that is,

$$\hat{y}_k = C\hat{x}_{k-1} + CBu_{k-1} + Du_k \tag{4.13}$$

$$y_k = \hat{y}_k + \varepsilon_k \tag{4.14}$$

$$\hat{u}_{f,k} = -F\hat{x}_k = -F(A\hat{x}_{k-1} + Bu_{k-1}) \tag{4.15}$$

$$u_{f,k} = \hat{u}_{f,k} + \eta_k \tag{4.16}$$

where the prediction errors ε_k and η_k are the differences between the estimated value and measurement for the output and feedback signal, respectively. Then one has

$$\begin{aligned}
\hat{y}_k &= C\hat{x}_{k-1} + CBu_{k-1} + Du_k \\
&= CA[\bar{x}_{k-1} + F_q(Y'_{q,k-1} - \bar{Y}'_{q,k-1})] + CBu_{k-1} + Du_k \\
&= CAF_q Y_{q,k-1} + CBu_{k-1} + CAF_q G_q U_{k-1} + CA(I_n - F_q H_q)\bar{x}_{k-1} + Du_k \\
&= \sum_{i=1}^{q} CAF_{q,i} y_{k-i} + Du_k + (CB - CAF_{q,1}D)u_{k-1} + \sum_{i=2}^{q} CAF_q G_{q,i} u_{k-i} + CAL\bar{x}_{k-1}
\end{aligned} \tag{4.17}$$

where $L = I_n - F_q H_q$, I_n an $n \times n$ identity matrix and $F_{q,i}$ and $G_{q,i}$ are the i-th partitions of F_q and G_q, respectively, defined as $F_q = [F_{q,1} \vdots F_{q,2} \vdots \cdots \vdots F_{q,q}]$,, $G_q = [G_{q,1} \vdots G_{q,2} \vdots \cdots \vdots G_{q,q}]$. Similar to (4.17), one can derive an ARX model to use one-step-ahead output prediction for $\hat{u}_{f,k}$

$$\begin{aligned}
\hat{u}_{f,k} &= -F\hat{x}_k = -F(A\hat{x}_{k-1} + Bu_{k-1}) \\
&= -FA\{\bar{x}_{k-1} + F_q(Y'_{q,k-1} - \bar{Y}'_{q,k-1})\} - FBu_{k-1} \\
&= -FA\bar{x}_{k-1} - FAF_q(Y_{q,k-1} + G_q U_{k-1}) + FAF_q H_q \bar{x}_{k-1} - FBu_{k-1} \\
&= -FA(I_n - F_q H_q)\bar{x}_{k-1} - FAF_q Y_{q,k-1} - FAF_q G_q U_{k-1} - FBu_{k-1} \\
&= -\sum_{i=1}^{q} FAF_{q,i} y_{k-i} - F(AF_q G_{q,1} + B)u_{k-1} - \sum_{i=2}^{q} FAF_q G_{q,i} u_{k-i} - FAL\bar{x}_{k-1}.
\end{aligned} \tag{4.18}$$

Equations (4.17) and (4.18) represent the optimal predictions of y_k and $u_{f,k}$ one can make using q previous input-output data. If the prediction is made once and for all, namely, no prediction of the previous state is made, the optimal value assigned to $\bar{x}_k$ is zero. However, if previous state estimation has been made, the optimal choice for $\bar{x}_k$ is the a priori Kalman filter estimate. Note that for a Kalman filter

$$\begin{aligned}\bar{x}_{k-1} &= A\bar{x}_{k-2} + AK(y_{k-2} - C\hat{x}_{k-2} - Du_{k-2}) + Bu_{k-2} + \cdots \\ &= \sum_{i=1}^{q-1} \bar{A}^{i-1} AKy_{k-1-i} + \sum_{i=1}^{q-1} \bar{A}^{i-1}(B - AKD)u_{k-1-i} + \bar{A}^q \hat{x}_{k-q} \end{aligned} \tag{4.19}$$

where $\bar{A} = A(I_n - KC)$ and K is the optimal steady state Kalman filter gain. Based on the argument above, one can replace $\bar{x}_{k-1}$ in (4.17) and (4.18) by (4.19) and obtain

$$\begin{aligned} y_k &= \hat{y}_k + \varepsilon_k \\ &= CAF_{q,1}y_{k-1} + \sum_{i=2}^{q} CA(F_{q,i} + L\bar{A}^{i-2}AK)y_{k-i} + Du_k + (CB - CAF_{q,1}D)u_{k-1} \\ &\quad + \sum_{i=2}^{q} CA(F_q G_{q,i} + L\bar{A}^{i-2}(B - AKD))u_{k-i} + \varepsilon_k + C\bar{A}^q \hat{x}_{k-q} \\ &= \sum_{i=1}^{q} a_i y_{k-i} + \sum_{i=0}^{q} b_i u_{k-i} + \varepsilon_k + C\bar{A}^q \hat{x}_{k-q} \end{aligned} \tag{4.20}$$

and $u_{f,k} = \hat{u}_{f,k} + \eta_k$

$$\begin{aligned} &= -FAL\left\{\sum_{i=1}^{q-1} \bar{A}^{i-1} AKy_{k-1-i} + \sum_{i=1}^{q-1} \bar{A}^{i-1}(B - AKD)u_{k-1-i} + \bar{A}^q \hat{x}_{k-q}\right\} \\ &\quad - \sum_{i=1}^{q} FAF_{q,i}y_{k-i} - \sum_{i=2}^{q} FAF_q G_{q,i}u_{k-i} - F(B + AF_q G_{q,1})u_{k-1} + \eta_k \\ &= -FAF_{q,1}y_{k-1} - \sum_{i=2}^{q} FA(F_{q,i} + L\bar{A}^{i-2}AK)y_{k-i} - F(B + AF_q G_{q,1})u_{k-1} \\ &\quad - \sum_{i=2}^{q} FA(F_q G_{q,i} + L\bar{A}^{i-2}(B - AKD))u_{k-i} - FAL\bar{A}^q \hat{x}_{k-q} + \eta_k \\ &= \sum_{i=1}^{q} c_i y_{k-i} + \sum_{i=1}^{q} d_i u_{k-i} + \eta_k - FAL\bar{A}^q \hat{x}_{k-q} \end{aligned} \tag{4.21}$$

Note that, although the steady-state Kalman filter gain might not be known at the very beginning, it has already existed. This implies that (4.20) and (4.21) are valid relations even for the very beginning of the data. In other words, once the value of every input-output term in (4.20) and (4.21) are known, these equations hold. Note that $\overline{A}$ in (4.19) is the system matrix of the Kalman filter dynamic equation. Equations (4.20) and (4.21) represent the ARX model of a linear system with process and measurement noises. These equations provide the optimal predictions of the output measurement and feedback signal at time k in the sense of minimum state error at time $k-1$ using q previous input and output data. For a stable filter, the matrix $\overline{A}$ is asymptotically stable. Therefore, the last term of (4.20) and (4.21) are negligibly small and can be neglected for a sufficiently large number q. It seems that these ARX models tend to be more accurate as q approaches to infinity. However, if q is too large, one will have overfitting problems[38] due to the prediction errors ε_k and η_k which are related to the process and measurement noises which may not be white or zero-mean.

4.3.2 Estimation of the ARX Model Coefficients

Estimation of the coefficient matrices of the ARX model given in (4.20) and (4.21) can be accomplished by using a least-square method. Equations (4.20) and (4.21) can be written in a compact matrix form:

$$\phi_q(k-1)\theta = z_k^T \tag{4.22}$$

where $\phi_q(k-1) = \begin{bmatrix} u_k^T & y_{k-1}^T & u_{k-1}^T & \cdots & y_{k-q}^T & u_{k-q}^T \end{bmatrix}$, $\theta = \begin{bmatrix} b_0 & a_1 & b_1 & \cdots & a_q & b_q \\ 0 & c_1 & d_1 & \cdots & c_q & d_q \end{bmatrix}^T$ and $z_k^T = \begin{bmatrix} y_k^T & u_{f,k}^T \end{bmatrix}$. The row vector $\phi_q(k-1)$ is called the regressor where q is the order-index and $k-1$ the time index, emphasizing the newest output vector, $y(k-1)$. Stacking up (4.22) for different k, one can form a matrix equation:

$$\begin{bmatrix} u_1^T & 0 & 0 & 0 & 0 & 0 \\ u_2^T & y_1^T & u_1^T & 0 & 0 & 0 \\ \vdots & \vdots & \vdots & \ddots & \vdots & \vdots \\ u_{q+1}^T & y_q^T & u_q^T & \cdots & y_1^T & u_1^T \\ \vdots & \vdots & \vdots & \ddots & \vdots & \vdots \\ u_k^T & y_{k-1}^T & u_{k-1}^T & \cdots & y_{k-q}^T & u_{k-q}^T \end{bmatrix} \theta = \begin{bmatrix} z_1^T \\ z_2^T \\ \vdots \\ z_{q+1}^T \\ \vdots \\ z_k^T \end{bmatrix}, \tag{4.23}$$

or in short,

$$\Phi_q(k-1)\theta = Z(k), \tag{4.24}$$

where $\Phi_q(k-1) \in R^{kxs}$ $(s=(m+p)q+m)$ denotes the data matrix while $Z(k)$ represents the output data and feedback input data matrix. One can use batch or recursive least-squares method to identify θ.

4.3.3 Markov Parameters from the ARX Model

In this section, the relationships between the system, Kalman filter and controller Markov parameters and the coefficient matrices of the ARX models will be derived. From (4.20) and (4.21), if the coefficient matrices of y_{k-j} and u_{k-j} are denoted by a_j, c_j, and b_j, d_j, respectively, one can derive

$$CA^jB = b_{j+1} + \sum_{i=1}^{j} a_i CA^{j-i}B + a_{j+1}D, \qquad j \geq 1 \tag{4.25}$$

$$-FA^jB = d_{j+1} + \sum_{i=1}^{j} c_i CA^{j-i}B + c_{j+1}D, \qquad j \geq 1. \tag{4.26}$$

These equations allow one to calculate the system Markov parameter CA^jB, and the controller Markov parameter $-FA^jB$ recursively from the coefficient matrices of an ARX model of order q (note that $D = b_0$, $CB = b_1 + a_1D$ and $-FB = d_1 + c_1D$). Here a proof of (4.26) is given and interested reader can find a proof of (4.25) in Ref. 6.

First, by definition, $G_{q,1} = \left[-D^T,\ 0^T,\ \cdots\ ,0^T\right]^T$, and for $j \geq 2$, one can have

$$G_{qj} = \begin{bmatrix} 0 \\ \vdots \\ 0 \\ CA^{-1}B - D \\ \vdots \\ CA^{-q+j-1}B \end{bmatrix} = \begin{bmatrix} C \\ \vdots \\ CA^{-j+2} \\ CA^{-j+1} \\ \vdots \\ CA^{-q+1} \end{bmatrix} A^{j-2}B - \begin{bmatrix} CA^{j-2} \\ \vdots \\ C \\ 0 \\ \vdots \\ 0 \end{bmatrix} B - \begin{bmatrix} 0 \\ \vdots \\ 0 \\ D \\ \vdots \\ 0 \end{bmatrix} = H_q A^{j-2}B - E^{(j-2)}B - D^{(j)} \quad (4.27)$$

where $E^{(j-2)} = \left[(CA^{j-2})^T,\ \cdots\ ,C^T\ \ ,0^T\ \ ,\cdots\ \ ,0^T\right]^T$,

$D^{(j)} = \left[0^T\ \ ,\cdots\ \ ,0^T\ \ ,D^T\ \ ,\cdots\ \ ,0^T\right]$,

($D^{(j)}$ has D in the j-th block and zero elsewhere).

Therefore, with $j \geq 1$

$$\begin{aligned} CAF_q G_{q,j+1} &= CAF_q H_q A^{j-1}B - CAF_q E^{(j-1)}B - CAF_{q,j+1}D \\ &= CAF_q H_q A^{j-1}B - \sum_{i=1}^{j} CAF_{q,i}CA^{j-i}B - CAF_{q,j+1}D \end{aligned} \quad (4.28)$$

Then using (4.21), (4.28), and the relations $\bar{A} + AKC = A$ and $F_q H_q + L = I_n$, one has

$$\begin{aligned} -FA^jB &= -FAA^{j-1}B = -FA(F_qH_q + L)A^{j-1}B = -FAF_qH_qA^{j-1}B - FALA^{j-1}B \\ &= -FAF_qH_qA^{j-1}B - FAL(\bar{A} + AKC)A^{j-2}B \\ &= -FAF_qH_qA^{j-1}B - FAL\bar{A}A^{j-2}B - FALAKCA^{j-2}B \\ &= \cdots\cdots \\ &= -FAF_qH_qA^{j-1}B - FAL\bar{A}^{j-2}AB - \sum_{i=1}^{j-2} FAL\bar{A}^{i-1}AKCA^{j-i-1}B \\ &= -FAF_qH_qA^{j-1}B - FAL\bar{A}^{j-2}(\bar{A} + AKC)B - \sum_{i=1}^{j-2} FAL\bar{A}^{i-1}AKCA^{j-i-1}B \\ &= -FAF_qH_qA^{j-1}B - FAL\bar{A}^{j-1}B - \sum_{i=1}^{j-2} FAL\bar{A}^{i-1}AKCA^{j-i-1}B - FAL\bar{A}^{j-2}AKCB \\ &= -FAF_qH_qA^{j-1}B + \sum_{i=1}^{j} FAF_{q,i}CA^{j-i}B + FAF_{q,j+1}D - FAL\bar{A}^{j-1}(B - AKD) \\ &\quad - \sum_{i=1}^{j} FAF_{q,i}CA^{j-i}B - \sum_{i=1}^{j-1} FAL\bar{A}^{i-1}AKCA^{j-i-1}B - FA(F_{q,j+1} + L\bar{A}^{j-1}AK)D \end{aligned}$$

$$
\begin{aligned}
&= -FAF_q G_{q,j+1} - FAL\bar{A}^{j-1}(B - AKD) - \sum_{i=1}^{j} FAF_{q,i} CA^{j-i} B \\
&\quad - \sum_{i=1}^{j-1} FAL\bar{A}^{i-1} AKCA^{j-i-1} B - FA(F_{q,j+1} + L\bar{A}^{j-1} AK) D \\
&= -FA\left(F_q G_{q,j+1} + L\bar{A}^{j-1}(B - AKD)\right) - FAF_{q,1} CA^{j-1} B - FA(F_{q,2} + LAK) CA^{j-2} B \\
&\quad - \cdots\cdots - FA(F_{q,j} + L\bar{A}^{j-2} AK) CB - FA(F_{q,j+1} + L\bar{A}^{j-1} AK) D \\
&= -FA\left(F_q G_{q,j+1} + L\bar{A}^{j-1}(B - AKD)\right) - FAF_{q,1} CA^{j-1} B \\
&\quad - \sum_{i=2}^{j} FA(F_{q,i} + L\bar{A}^{i-2} AK) CA^{j-i} B - FA(F_{q,j+1} + L\bar{A}^{j-1} AK) D \\
&= d_{j+1} + \sum_{i=1}^{j} c_i CA^{j-i} B + c_{j+1} D. \qquad (4.29)
\end{aligned}
$$

Similar to (4.25) and (4.26), there are another two equations to obtain the Kalman filter Markov parameter $CA^{j+1}K$ and the Kalman filter/controller Markov parameter $-FA^{j+1}K$ recursively from the coefficient matrices of the ARX models as follows:

$$
CA^{j+1}K = a_{j+1} + \sum_{i=1}^{j} a_{j-i+1} CA^i K, \qquad j \geq 1 \qquad (4.30)
$$

$$
-FA^{j+1}K = c_{j+1} + \sum_{i=1}^{j} c_{j-i+1} CA^i K, \qquad j \geq 1. \qquad (4.31)
$$

Note that $CAK = a_1$ and $-FAK = c_1$. Here a proof of (4.30) is given and one can derive (4.31) in a similar way. Using (4.20) and the relations $\bar{A} + AKC = A$, and $F_q H_q + L = I_n$, one has

$$
\begin{aligned}
CA^{j+1}K &= CA(F_q H_q + L)A^j K = CAF_q H_q A^j K + CALA^j K \\
&= CA(F_{q,j+1} + F_{q,j} CA^{-j+1} A^j K + F_{q,j-1} CA^{-j+2} A^j K + \cdots + F_{q,1} CA^j K) \\
&\quad + CA(L\bar{A}A^{j-1} K + LAKCA^{j-1} K) \\
&= \cdots \\
&= CA(F_{q,j+1} + F_{q,j} CAK + F_{q,j-1} CA^2 K + \cdots + F_{q,1} CA^j K) \\
&\quad + CA(L\bar{A}^{j-1} AK + L\bar{A}^{j-2} AKCAK + \cdots + CAL\bar{A}AKCA^{j-2} K + CALAKCA^{j-1} K) \\
&= CAF_{q,j+1} + \sum_{i=1}^{j} CAF_{q,j-i+1} CA^i K + CAL\bar{A}^{j-1} AK + \sum_{i=1}^{j-1} CAL\bar{A}^{j-i-1} AKCA^i K
\end{aligned}
$$

$$= CA(F_{q,j+1} + L\bar{A}^{j-1}AK) + \sum_{i=1}^{j} CA(F_{q,j-i+1} + L\bar{A}^{j-i-1}AK)CA^iK$$

$$= a_{j+1} + \sum_{i=1}^{j} a_{j-i+1}CA^iK . \qquad (4.32)$$

4.3.4 Realization of System, Kalman Filter and Controller Gains

To decompose the identified Markov parameters into the open-loop state-space model, Kalman and controller gains, one can use a realization algorithm like the Eigensystem Realization Algorithm (ERA).[17] There are two possible approaches. In the first approach, one may use the combined Markov parameters shown in (4.25), (4.26), (4.30) and (4.31) to form a Hankel matrix to compute a realization of the open-loop state-space model, Kalman and controller gains at the same time.[11] The second approach is to realize the open-loop state-space model, Kalman and controller gains separately. The system Markov parameters shown in (4.25) can be used to form a Hankel matrix to realize the open-loop state-space model. Then the Kalman gain is identified from the Kalman filter Markov parameter shown in (4.30) and the identified open-loop state-space model through least-squares. This approach has been used in Ref. 6. Similarly, the controller gain can be identified from the controller Markov parameter shown in (4.26) and the identified open-loop state-space model through least-squares. Here the second approach is shortly shown to get the open-loop state-space model and Kalman filter gain.

The open-loop state-space model can be realized from the open-loop system Markov parameters through the Singular Value Decomposition (SVD) method.[17,25] The first step is to form a Hankel matrix from the open-loop system Markov parameters,

$$H(j)=\begin{bmatrix} Y(j) & Y(j+1) & \cdots & Y(j+\beta) \\ Y(j+1) & Y(j+2) & \cdots & Y(j+\beta+1) \\ \vdots & \vdots & \ddots & \vdots \\ Y(j+\gamma) & Y(j+\gamma+1) & \cdots & Y(j+\gamma+\beta) \end{bmatrix}, \tag{4.33}$$

where $Y(j)$ is the j-th Markov parameter. From the measurement Hankel matrix, the realization uses the SVD of $H(1)$, $H(1)=U\Sigma V^T$, to identify a n-th order discrete state-space model as

$$A=\Sigma_n^{-1/2}U_n^T H(2)V_n\Sigma_n^{-1/2},\ B=\Sigma_n^{1/2}V_n^T E_s,\ C=E_m^T U_n\Sigma_n^{1/2}, \tag{4.34}$$

where matrix Σ_n is the upper left hand $n\times n$ partition of Σ containing the n largest singular values along the diagonal. Matrices U_n and V_n are obtained from U and V by retaining only the n columns of singular vectors associated with the n singular values. Matrix E_m is a matrix of appropriate dimension having m columns, all zero except that the top $m\times m$ partition is an identity matrix. E_s is defined similarly. Once the open-loop A and C are obtained, one can easily calculate the open-loop Kalman filter gain from the open-loop Kalman filter Markov parameters $N(k)$ in a least-squares sense as follows

$$K=(O^TO)^{-1}O^T\begin{bmatrix} N(1) \\ : \\ N(k) \end{bmatrix},\ \text{where } O=\begin{bmatrix} CA \\ : \\ CA^k \end{bmatrix}. \tag{4.35}$$

The identified Kalman filter gain can be used directly for state estimation.

4.4 Numerical Examples and Experimental Results

In order to demonstrate the feasibility of the method developed in this chapter, numerical simulations and test data from the Large-Angle Magnetic Suspension Test Facility (see Fig. 3.1) are used. In the numerical simulations, the optimal ARX order problem and the

advantage of combining any Markov parameters shown in (4.26), (4.30) and (4.31) with the system Markov parameter shown in (4.25) to realize the open-loop state-space model are studied. First, it is noted that the ARX models shown in (4.20) and (4.21) seem to be more accurate as q approaches infinity. However, if q is too large, there will be overfitting problems. Numerical simulations are performed to verify this by using the analytical model shown in Chapter 3. A full state feedback controller based on the linear quadratic regulator design is used to stabilize the open-loop system. Two different noise levels (0.5% and 2.5%) for both process and measurement noise are studied.

The identified A_{21}, A_{22}, and B_2 matrices from Case 4 with 0.5% noise in the numerical simulations are

$$\hat{A}_{21} = \begin{bmatrix} 3338.3 & -0.3874 & -39289 & -57.355 & -57.355 \\ 5.2490 & 3340.4 & -287.86 & 200.09 & -357.40 \\ -9.7983 & 0.0113 & 50.452 & -1.9976 & 0.2824 \\ -0.2054 & 0.0009 & 0.4265 & 95.975 & -0.6959 \\ 0.001 & 0.0086 & 0.5742 & -0.6424 & 0.1043 \end{bmatrix},$$

$$\hat{A}_{22} = \begin{bmatrix} 0.0074 & -0.0072 & -4.0923 & 2.1736 & 3.1025 \\ -0.1057 & -0.0229 & 5.7476 & 19.492 & -4.2297 \\ -0.0000 & -0.0000 & -0.0176 & 0.0911 & 0.0513 \\ 0.0000 & -0.0000 & 0.0561 & 0.0152 & -0.0204 \\ -0.0000 & -0.0000 & 0.0375 & -0.0046 & -0.0389 \end{bmatrix},$$

$$\hat{B}_2 = \begin{bmatrix} 38.363 & 38.353 & 38.329 & 38.375 & 38.352 \\ -0.0253 & 89.859 & 55.426 & -55.541 & -89.715 \\ 0.2227 & -0.1526 & 0.0789 & 0.0770 & -0.1522 \\ -0.0012 & 0.1213 & -0.1967 & 0.1962 & -0.1215 \\ -0.2773 & -0.0854 & 0.2241 & 0.2236 & -0.0856 \end{bmatrix}.$$

There are 6000 data points with 10 ms sampling time and the number of Markov parameters used for ERA is 25. Tables 1 and 2 show the error percentage of the first 30

system Markov parameters for the two different noise levels, respectively. The error percentage is defined as

$$e = \frac{\left\| CA^i B - \hat{C}\hat{A}^i \hat{B} \right\|_2}{\left\| CA^i B \right\|_2} \times 100\%. \tag{4.36}$$

For Case 1 in both tables, the combined four Markov parameters shown in (4.25), (4.26), (4.30) and (4.31) are used to realize the system model through ERA. For Case 2, only the system and controller Markov parameters are used. For Case 3, only the system and Kalman filter Markov parameters are used. For Case 4, only the system Markov parameter is used. The identified model (after the coordinate transformation) from Case 4 with 0.5% noise is shown in appendix. The result is very close to the analytical model.

From the simulations, it is observed that the optimal order of the ARX model is 7 for the 0.5% noise case and 8 for the 2.5% case. If higher order is used, the identified system Markov parameter will be less accurate. Further investigation is needed to clarify the relation between the optimal ARX order and the noise level. As the results for the four cases are compared, it is shown that there is no clear advantage to combine any Markov parameters shown in (4.26), (4.30) and (4.31) with the system Markov parameter to realize the open-loop system. Figure 4.3 shows the comparison of the (1,1) element of the true and reconstructed Markov parameter matrices of $CA^{i-1}B$, $CA^{i-1}AK$, $FA^{i-1}B$ and $FA^{i-1}AK$. The result is obtained for Case 1 with 2.5% noise and the ARX model order is 8. The error becomes larger for each Markov parameter as the power index i increases.

For the experiment, a full state feedback controller based on the linear quadratic regulator design is also used to stabilize the open-loop system. However, since only five position sensors are available, the rate information are calculated from the back difference of the position signals. There are 6000 data points with 4 ms sampling time and the number of

Markov parameters used for ERA is 60. Different ARX model orders are used. Since the simulations show that there is no clear advantage of combining any other Markov parameters with the system Markov parameter, only the system Markov parameter is used for realization. After obtaining the identified model from the test data, the identified model is evaluated by using another feedback controller which gives low damping for the closed-loop system. The simulated closed-loop step responses from the identified model and the analytical model are compared with the test data. Figure 4.4 shows the error percentage of the first 0.1 second step response verse the ARX model order. The error percentage is defined in (4.36) and the system Markov parameter is replaced by the step response signal. The result shows that the optimal order is about 12. Figure 4.5 shows the step responses of the testing data, analytical model and identified model for a yaw step command. Both the test data and identified model show that the yaw motion is coupled with the pitch and demonstrates a low damping as one expects. However, the analytical model fails to predict both characteristics.

4.5 Concluding Remarks

In this chapter, projection filters are developed to identify an open-loop stochastic system operating under closed-loop condition. The main contribution in the algorithm developed here is that open-loop system, Kalman filter and controller Markov parameters are recursively derived without feedback dynamics from the ARX model coefficients of the closed-loop input-output data. Numerical simulations for an unstable Large-Angle Magnetic Suspension Test Facility show that there exists an optimal ARX order for the realization of the state-space model which is related to the level of the noise. There is no clear advantage to combine any other Markov parameters with the system Markov parameter to realize the open-loop system. Closed-loop test data demonstrate that the open-loop state-space model

identified by using the projection filters is fairly accurate in predicting the step responses while the analytical model has several deficiencies.

Table 4.1 Error percentage of system Markov parameter for 0.5% noise

Order of ARX	Case 1	Case 2	Case 3	Case 4
2	1.6542	1.6542	1.6542	1.6542
3	0.8294	0.8248	0.8573	0.8248
4	0.7267	0.7243	0.7314	0.7243
5	0.7144	0.7098	0.7067	0.7098
6	0.6978	0.7016	0.7135	0.7016
7	0.6840	0.6892	0.7136	0.6892
8	0.6849	0.7027	0.7424	0.7027
9	0.7264	0.7301	0.7638	0.7300
10	0.7205	0.7198	0.7148	0.7198

Table 4.2 Error percentage of system Markov parameter for 2.5% noise

Order of ARX	Case 1	Case 2	Case 3	Case 4
4	5.6100	5.6100	5.6057	5.6100
6	4.0671	4.0666	4.0730	4.0667
7	3.9216	3.9224	3.9269	3.9224
8	3.7410	3.7470	3.7519	3.7469
9	3.8866	3.8936	3.9081	3.8940
10	4.0368	4.0419	4.0615	4.0425

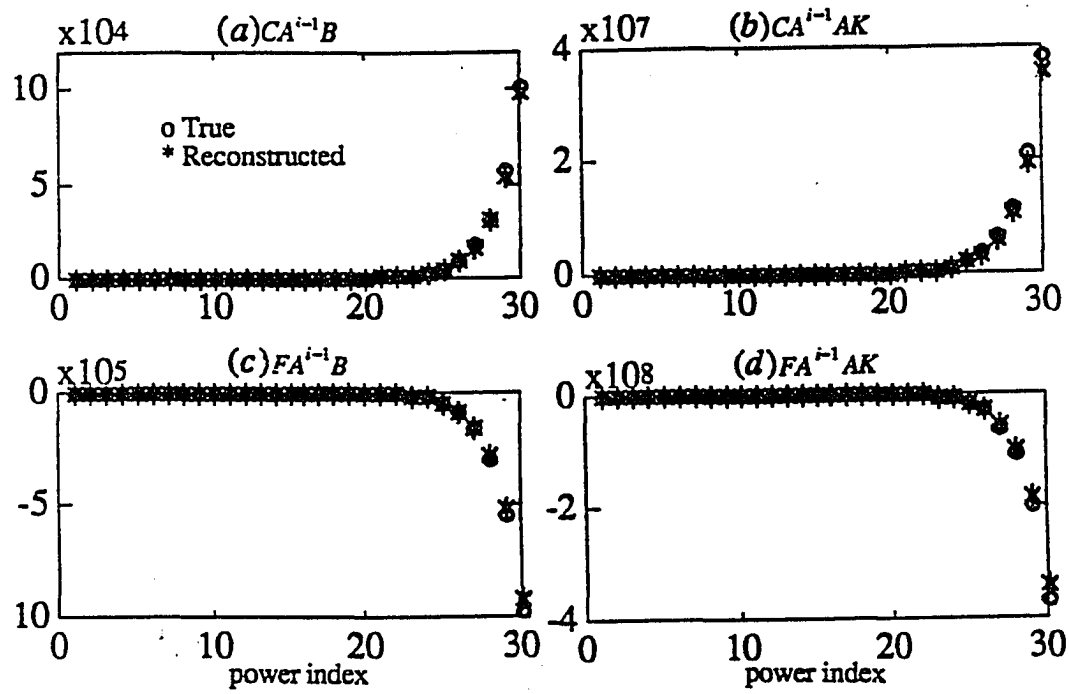

Fig. 4.3 Comparison of identified Markov parameter sequence ((1,1) element) with its true value. (a) $CA^{i-1}B$, (b) $CA^{i-1}AK$, (c) $FA^{i-1}B$ and (d) $FA^{i-1}AK$.

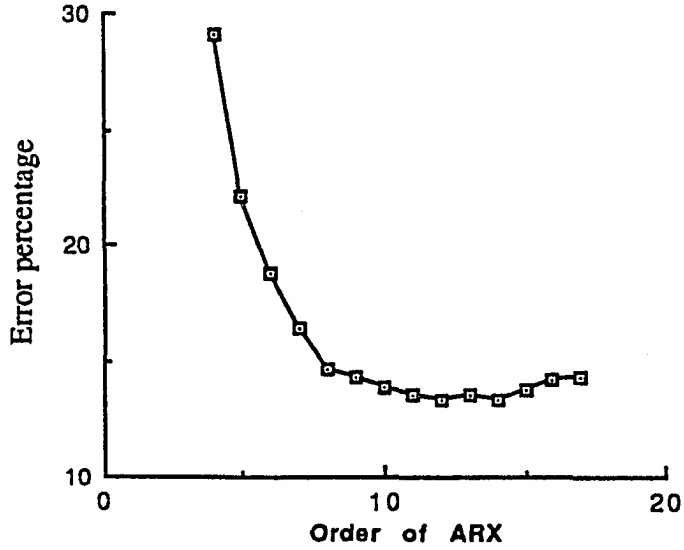

Fig. 4.4 Error percentage of step response for the identified model.

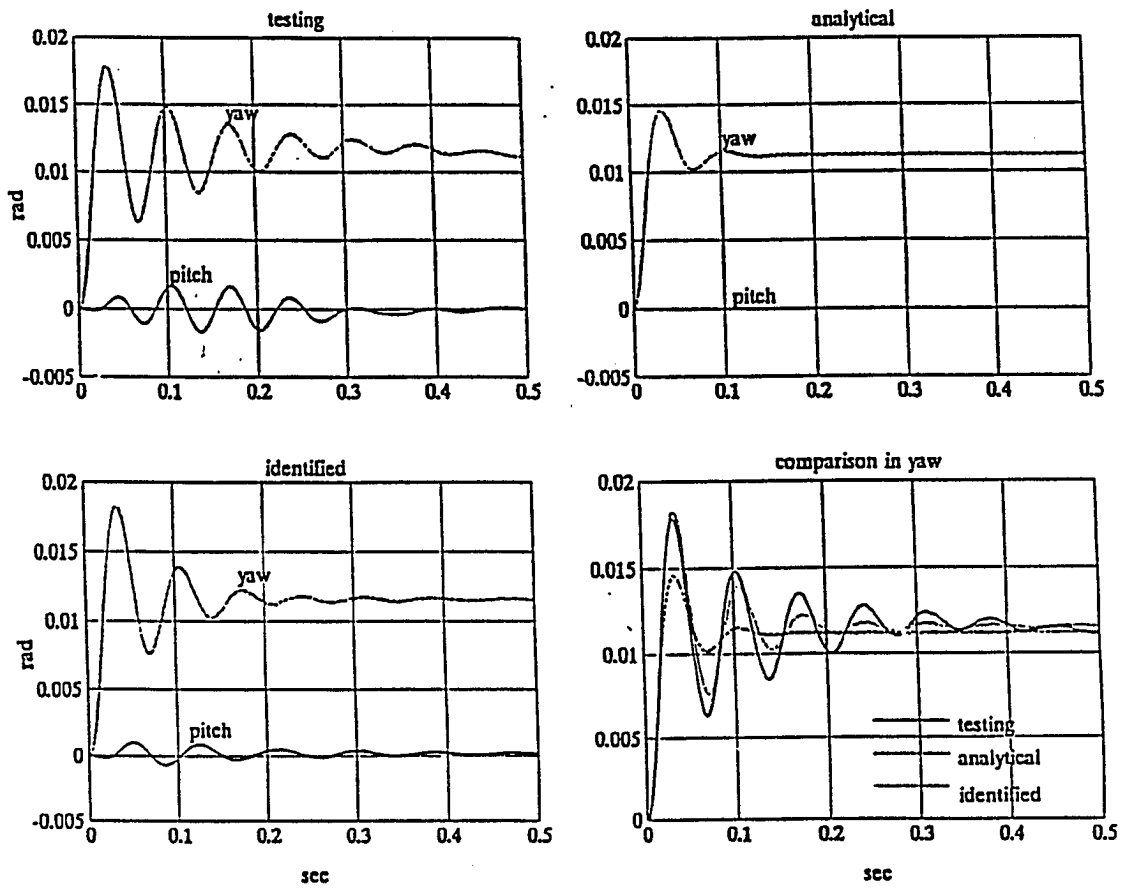

Fig. 4.5 The step response from testing, analytical, and identified model for the yaw step.

Chapter 5

FREQUENCY DOMAIN CLOSED-LOOP IDENTIFICATION

5.1 Introduction

The frequency domain approach has dominated the structural engineering literature on modal testing for many years. In the vast majority of modal testing, frequency response functions are measured prior to using a modal identification algorithm. Therefore, many system identification methods available today are based on the use of frequency response functions. Classical identification of linear systems for model verification and control design is commonly performed using concepts from spectral analysis. Often in practice, sophisticated spectrum analyzers are used to acquire measurements of structural dynamics. Since stability and performance of a control system can be efficiently captured in the frequency domain, the construction of an accurate model directly from frequency domain data is of particular interest to active control applications. The objective of frequency domain state-space system identification is to identify state-space models from the given frequency data - the frequency response function (FRF).

Classically, the Inverse Discrete Fourier Transform method (IDFT) is used to transform frequency response data to time domain data, that is, to transform the frequency response function (FRF) of the system to its pulse response. The pulse response of discrete-time systems is also known as the Markov parameters. The disadvantage of this approach is that the Markov parameter sequence thus obtained is distorted by time-aliasing effects[39]. Recently, a method called the State-Space Frequency Domain (SSFD) identification algorithm has been developed.[16,19] In Ref. 16, Markov parameters can be calculated from FRF without windowing distortion and an arbitrary frequency weighting can be introduced to shape the estimate error. The method uses a rational matrix function to curve-fit frequency data and obtains the Markov parameters from this equation. The disadvantage of this method is that curve-fitting problem must either be solved by non-linear optimization techniques or by linear approximate algorithms requiring several iterations. In Ref. 19, the method uses a matrix-fraction for the curve fitting and the curve-fitting is reformulated as a linear problem which can be solved by the ordinary least-squares method in one step; that is, no iteration is required. This approach is similar to SSFD and thus retains all the advantages associated with SSFD while avoiding the iterative, approximate curve-fitting procedures. The method is derived for open-loop systems which do not involve feedback dynamics.

As discussed earlier in chapter 2, it is generally harder to identify the open-loop system from the open-loop input-output data because it is difficult to ensure that the input signal to the plant has sufficient frequency richness to excite all of the system's dynamics. Recently, a method has been proposed to identify open-loop system from closed-loop input-output data with known feedback dynamics in *time* domain.[24] The method developed in this chapter is a natural extension of the closed-loop identification method to *frequency* domain and can be used to identify a linear open-loop stochastic system from *closed-loop* input-output data and known feedback dynamics in *frequency* domain.

On the other hand, the ultimate goal of a control system designer is to build a system that will work in the real environment. Because the real environment may change with time (components may age or their parameters may vary with temperature or other environmental condition), or operating conditions may vary (load changes, disturbances), the control system must be able to withstand these variations, which is called structured uncertainty. Even if the environment does not change, there is another source of uncertainty in modeling. Any mathematical representation of a system often involves simplifying assumptions. Nonlinearities are either unknown and hence unmodeled, or modeled and later ignored to simplify analysis. Different components of systems (actuators, sensors, amplifiers, motors, gears, belts, etc.) are sometimes modeled by constant gains, even though they may have dynamics or nonlinearities. Dynamic structures (e.g., aircraft, satellites, missiles) have complicated high frequency dynamics that are often ignored at the design stage. Because control systems are typically designed using much-simplified models of systems, there are always discrepancies between true and modeled models. The difference is called unstructured uncertainty and the model may not work on the real plant in real environments.

The particular property that a control system must possess for it to operate properly in realistic situations is called *robustness*. The problem of designing controllers that satisfy robust stability and performance requirements is called *robust control*. A variety of approaches to this problem was investigated intensely during the 1980s and is still under investigation by many researchers.[20] The LAMSTF model was also used to design robust controllers to improve the robustness[40,41] but no attempt was made to characterize the uncertainty in the analytical model or the identified model from test data. A simulation model is proposed by comparing the maximum singular value of the uncertainty models. Also by comparing FRFs for the different number of modes, a method to find a appropriate number of states mode will be discussed.

In this chapter, the relation between the FRF and the closed-loop system and Kalman filter Markov parameters is derived for stochastic systems. Once the closed-loop system and Kalman filter Markov parameters are obtained from FRF, a *recursive* formula for computing the open-loop system and Kalman filter Markov parameters from the closed-loop system, Kalman filter and controller Markov parameters can be used. Finally, the open-loop system can be realized from the calculated open-loop system Markov parameters. The method can also estimate the Kalman filter gain directly without estimating noise covariances.

5.2 Open-loop State-space and FRF Relationship

The Frequency Response Function (FRF) is defined as the Fourier transform of impulse or pulse response function sequence (Markov Parameters). The dynamic characteristics of a linear time invariant stable system can be sufficiently described by a frequency response function. The frequency response function is simply a special case of the transfer function but, in practice, it may replace the transfer function with no loss of useful information. In the majority of testing, frequency response functions are computed prior to using an identification algorithm. There are many reasons why FRFs are still generated so often, although there are many identification algorithms available which can analyze free or forced response time histories directly. Experienced modal testing personnel can deduce considerable information simply by observing frequency response functions. If time histories are processed directly by the modal identification algorithm, many traditional evaluation criteria are unavailable.

The state-space representation of a finite-dimensional, linear, discrete-time, time-invariant system can be modeled as:

$$x_{k+1} = Ax_k + Bu_k \tag{5.1}$$

$$y_k = Cx_k \,, \tag{5.2}$$

where $x \in R^{n\times 1}$, $u \in R^{r\times 1}$, $y \in R^{m\times 1}$ are state, input and output vectors, respectively; $[A,\ B,\ C]$ are the system matrix, input matrix and output matrix, respectively. $[A,\ B,\ C]$ are referred to as state-space parameters or the state-space model. The relation between the state-space model and the FRF $G(\omega_i)$ is

$$G(\omega_i) = C\left(e^{j\omega_i T} \times I_n - A\right)^{-1} B \tag{5.3}$$

where T is the sampling time of the discrete time system in seconds and ω_i are the frequencies in rad/sec. By expanding (5.3), one has

$$G(\omega_i) = CBe^{-j\omega_i T} + CABe^{-j\omega_i T} + CA^2Be^{-j\omega_i T} + \cdots = \sum_{k=0}^{\infty} Y_k e^{-jk\omega_i T} \tag{5.4}$$

$$\left(Y_k = CA^{k-1}B\right)$$

The parameters $\left(Y_k = CA^{k-1}B\right)$ $(k = 1,2,\cdots,\infty)$ are the Markov parameters. However, the problem associated with this approach is that theoretically the Markov parameters have an infinite number of terms. Though overall the Markov sequence is a decreasing sequence, assuming the system is stable, it may take a large truncation number k_1 to make $CA^{k-1}B \approx 0$ for all $k \geq k_1$, especially when the system is lightly damped. A large number of Markov parameters will make computation too intensive and impractical for many applications. To avoid this problem of excessive number of parameters in the calculation, an intermediate step should be taken. That is, curve-fit the FRF data using a finite-ordered matrix-fraction first and then construct the Markov parameters from this results.

5.3 The Relation between Closed-Loop State-Space and FRF

This time, a finite-dimensional, linear, discrete-time, time-invariant system with processing and measurement noises is modeled as:

$$x_{k+1} = Ax_k + Bu_k + w_k \tag{5.5}$$

$$y_k = Cx_k + v_k\,, \tag{5.6}$$

where w_k is the process noise, v_k the measurement noise. Sequences w_k and v_k are assumed Gaussian, white, zero-mean, and stationary with covariance matrices Q and R respectively. One can derive a steady-state filter innovation model:[26]

$$\hat{x}_{k+1} = A\hat{x}_k + Bu_k + AK\varepsilon_k \tag{5.7}$$

$$y_k = C\hat{x}_k + \varepsilon_k\,, \tag{5.8}$$

where $\hat{x}_k$ is the a priori estimated state, K is the steady-state Kalman filter gain and ε_k is the residual after filtering: $\varepsilon_k = y_k - C\hat{x}_k$. The existence of K is guaranteed if the system is detectable and $(A, Q^{1/2})$ is stabilizable.[27]

On the other hand, a dynamic output feedback controller can be modeled as:

$$p_{k+1} = A_d p_k + B_d y_k \tag{5.9}$$

$$u_k = C_d p_k + D_d y_k + r_k, \tag{5.10}$$

where A_d, B_d, C_d, and D_d are the system matrices of the dynamic output feedback controller; $p \in R^{l\times 1}$, $r \in R^{s\times 1}$ are controller state and reference input to the closed-loop system. Combining (5.7) to (5.10), the augmented closed-loop system dynamics becomes

$$\eta_{k+1} = A_c\eta_k + B_c r_k + A_c K_c \varepsilon_k \tag{5.11}$$

$$y_k = C_c\eta_k + \varepsilon_k, \tag{5.12}$$

where

$$\eta_k = \begin{bmatrix} \hat{x}_k \\ p_k \end{bmatrix}, A_c = \begin{bmatrix} A + BD_d C & BC_d \\ B_d C & A_d \end{bmatrix}, B_c = \begin{bmatrix} B \\ 0 \end{bmatrix},$$

$$A_c K_c = \begin{bmatrix} AK + BD_d \\ B_d \end{bmatrix}, \text{and } C_c = [C \quad 0].$$

It is noted that K_c can be considered as the Kalman filter gain for the closed-loop system and the existence of the steady-state K_c is guaranteed when the closed-loop system matrix A_c is nonsingular. Substituting (5.12) into (5.11) yields

$$\eta_{k+1} = \overline{A}\eta_k + B_c r_k + A_c K_c y_k \,, \tag{5.13}$$

where $\overline{A} = A_c - A_c K_c C_c$ and is guaranteed to be asymptotically stable because the steady-state Kalman filter gain K_c exists. The z-transform of (5.12) and (5.13) yield

$$y(z) = C_c \eta(z) + \varepsilon(z) \tag{5.14}$$

$$\eta(z) = (zI_t - \overline{A})^{-1}(A_c K_c y(z) + B_c r(z)) \,, \tag{5.15}$$

where I_t is an identity matrix with dimension $t = n + l$. Substituting (5.15) into (5.14), one has

$$y(z) = C_c(zI_t - \overline{A})^{-1}(A_c K_c y(z) + B_c r(z)) + \varepsilon(z) \,. \tag{5.16}$$

By rearranging, one has

$$\begin{aligned} y(z) = {} & (I_m - C_c(zI_t - \overline{A})^{-1} A_c K_c)^{-1} C_c (zI_t - \overline{A})^{-1} B_c r(z) \\ & + (I_m - C_c(zI_t - \overline{A})^{-1} A_c K_c)^{-1} \varepsilon(z) \,. \end{aligned} \tag{5.17}$$

The z-transform of the dynamic output feedback controller (5.9) and (5.10) and the closed-loop state-space model (5.11) and (5.12) yield

$$u(z) = \sum_{k=0}^{\infty} Y_d(k) z^{-k} y(z) + r(z) \,, \tag{5.18}$$

$$y(z)=\sum_{k=1}^{\infty}Y_c(k)z^{-k}r(z)+\sum_{k=0}^{\infty}N_c(k)z^{-k}\varepsilon(z)\,, \tag{5.19}$$

where $Y_d(k)=C_dA_d^{k-1}B_d$ is the controller Markov parameter, $Y_c(k)=C_cA_c^{k-1}B_c$ the closed-loop system Markov parameter, and $N_c(k)=C_cA_c^{k-1}A_cK_c$ the closed-loop Kalman filter Markov parameters. It is also noted that $Y_d(0)=D_d$ and $N_c(0)=I$.

The transfer function matrix of the system described by Eq.(5.17) is

$$G(z^{-1})=(I_m-C_c(zI_t-\overline{A})^{-1}A_cK_c)^{-1}C_c(zI_t-\overline{A})^{-1}B_c=\sum_{k=1}^{\infty}Y_c(k)z^{-k}\,. \tag{5.20}$$

The FRF is simply the transfer function matrix $G(z^{-1})$ calculated along the unit circle in the z plane. It is also chosen that the transfer function matrix can be expressed by a left-fraction description as[19]

$$G(z^{-1})=\alpha^{-1}(z^{-1})\beta(z^{-1})\,, \tag{5.21}$$

where both $\alpha(z^{-1})$ and $\beta(z^{-1})$ are matrix polynomials,

$$\alpha(z^{-1})=I_m+\alpha_1z^{-1}+\cdots+\alpha_pz^{-p}\,, \tag{5.22}$$

$$\beta(z^{-1})=\beta_1z^{-1}+\cdots+\beta_pz^{-p}\,. \tag{5.23}$$

The factorization is also not unique. For convenience one can choose the orders of both polynomials to be equal ($=p$). Pre-multiplying (5.21) by $\alpha(z^{-1})$ one has

$$\alpha(z^{-1})G(z^{-1})=\beta(z^{-1})\,, \tag{5.24}$$

which can be rearranged to become

$$G(z^{-1})=-\alpha_1G(z^{-1})z^{-1}-\cdots-\alpha_pG(z^{-1})z^{-p}+\beta_1z^{-1}+\cdots+\beta_pz^{-p}\,, \tag{5.25}$$

α and β can be found by least-squares method. Eq. (5.24) can be written as

$$\left(\sum_{i=0}^{p}\alpha_i z^{-i}\right)\left(\sum_{i=0}^{\infty}Y_c(i)z^{-i}\right)=\sum_{i=1}^{p}\beta_i z^{-i}\ . \tag{5.26}$$

From this relation, the closed-loop system Markov parameters can be recursively calculated from the estimated α and β matrix polynomials by using the parameter convolution of polynomial products as follows:

$$Y_c(k)=\beta_k-\sum_{i=1}^{k}\alpha_i Y_c(k-i)\ . \tag{5.27}$$

Similarly, the closed-loop Kalman filter Markov parameters can be recursively calculated from the estimated α matrix polynomials as follows:

$$N_c(k)=-\sum_{i=1}^{k}\alpha_i N_c(k-i)\ . \tag{5.28}$$

Then, one can recursively calculate the open-loop system and Kalman filter Markov parameters from the closed-loop system, Kalman filter Markov parameters , and the known controller Markov parameters by the following relations as was discussed in Chapter 2.

$$Y(j)=Y_c(j)-\sum_{k=1}^{j}\sum_{i=1}^{k}Y(i)Y_d(k-i)Y_c(j-k) \tag{5.29}$$

$$N(j)=N_c(j)-\sum_{k=1}^{j}\sum_{i=1}^{k}Y(i)Y_d(k-i)N_c(j-k). \tag{5.30}$$

where $Y(k)=CA^{k-1}B$ is the open-loop system Markov parameter,

$N(k)=CA^{k-1}AK$ open-loop Kalman filter Markov parameter,

$N(0)=I$ which is an identity matrix,

$Y_d(k)=C_dA_d^{\,k-1}B_d$ the controller Markov parameter,

$Y_c(k)=C_cA_c^{\,k-1}B_c$ the closed-loop system Markov parameter, and

$N_c(k)=C_cA_c^{\,k-1}A_cK_c$ the closed-loop Kalman filter Markov parameters.

It is also noted that $Y_d(0)=D_d$, $N_c(0)=I$ and $Y_c(0)=0$.

To decompose the identified Markov parameters into the open-loop state-space model, Kalman and controller gains, one can use a realization algorithm like the Eigen Realization Algorithm (ERA) which was explained in Chapter 4. Finally, the procedures for identifying an open-loop state-space model from closed-loop input-output data with a known dynamic output feedback controller can be summarized as follows.

1. Obtain FRF from closed-loop input-output data by using (5.17).
2. Use least-square method to compute left-fraction matrix polynomials from the FRF by using (5.25).
3. Compute closed-loop system and Kalman filter Markov parameters recursively using the left-fraction matrix polynomials by using (5.27),(5.28).
4. Compute the open-loop system and Kalman filter Markov parameters from the closed-loop system and Kalman filter Markov parameters, and the controller Markov parameters calculated from the known controller dynamics by using (5.29),(5.30)
5. Realize open-loop system matrices from the open-loop system Markov parameters by using (4.37), (4,38).
6. Estimate open-loop Kalman filter gain from the open-loop Kalman filter Markov parameters and the realized system matrices by using (4.39).

5.4 Model Uncertainty

A stable system is not our final objective, however, *robust* is; stability must be maintained despite model *uncertainty*. This is a subject of much current research interest. It has been widely recognized that not every controller suited for the nominal model will perform equally well with the plant. The general principle is that robustness must be traded off versus nominal performance. This involves two complementary prerequisites:

- The controller must be robust for the imperfections of the nominal model, and
- these imperfections must allow the design of a high performance controller.

The first prerequisite shows the need of a quantified (bound on the) model uncertainty, whereas the second one refers to the construction of a sufficiently accurate or suitable nominal model, as a basis for the control design. Accordingly, the field of control-relevant system identification branches into two directions as depicted in Figure 5.1.

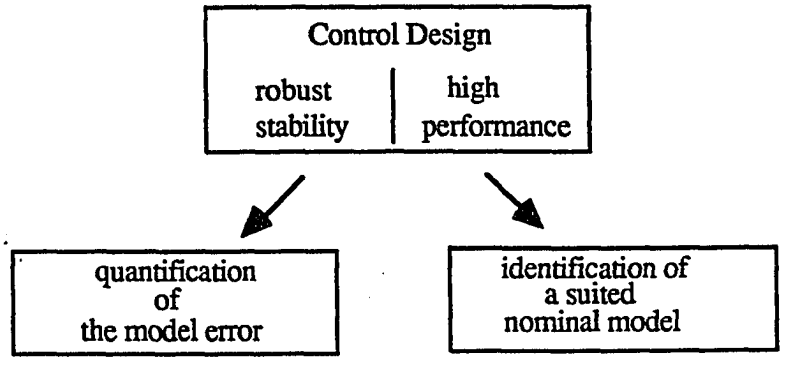

Figure 5.1 The two branches of control-relevant system identification

Model uncertainty is generally divided into two categories: structured uncertainty and unstructured uncertainty. Structured uncertainty assumes that the uncertainty is modeled, and we have ranges and bounds for uncertain parameters in the system. Unstructured uncertainties assume less knowledge of the system. We only assume that the frequency response of the system lies between two bounds. Both kinds of uncertainties are usually present in most applications. For the NASA LAMSTF, it is found that for the baseline system the analytic model nearly captures the dynamics, although the identified model improves the simulation accuracy. For the system perturbed by additional eddy currents which is shown in Figure 5.2, the analytic model is no longer adequate and a higher-order model, determined through system identification, is required to accurately predict the system's response.[42]

5.5 Numerical and Test Example

An example is provided which consists of numerical simulations and actual hardware tests to validate the feasibility of the proposed closed-loop identification method. As an example, LAMSTF of Chapter 3 would be used again. Because it is difficult to accurately model the magnetic field and its gradients, the analytical model needs to be improved through identification from experimental data. The discrete-time state-space parameters of (5.5) and (5.6) using a sampling rate of 250 Hz are listed in Appendix A. The measured voltage outputs by y are related to physical states y' by

$$y' = [s2p]y, \quad y = [p2s]y' \tag{5.31}$$

Both the sensor (physical states to output voltage) and actuator systems (current to forces and torques) have high bandwidth and are modeled as constants denoted by matrices $s2p$, $p2s$ and $a2f$ as followings:

$$s2p = \begin{bmatrix} -0.0349 & 0.0349 & 0 & 0 & 0 & 0 \\ 0 & 0 & -0.0167 & -0.0167 & 0.0167 & 0.0167 \\ 0 & 0 & 0.0004 & -0.0004 & -0.0004 & 0.0004 \\ 0 & 0 & -0.0004 & 0.0004 & -0.0004 & 0.0004 \\ 0.0006 & 0.0006 & 0 & 0 & 0 & 0 \end{bmatrix}$$

$$p2s = \begin{bmatrix} -14.3200 & 0 & 0 & 0 & 800.0000 \\ 14.3200 & 0 & 0 & 0 & 800.0000 \\ 0 & -14.9884 & 565.6000 & -565.6000 & 0 \\ 0 & -14.9884 & -565.6000 & 565.6000 & 0 \\ 0 & 14.9884 & -565.6000 & -565.6000 & 0 \\ 0 & 14.9884 & 565.6000 & 565.6000 & 0 \end{bmatrix}$$

$$a2f = \begin{bmatrix} 0.0002 & 0.0002 & 0.0002 & 0.0002 & 0.0002 \\ 0 & 0.0005 & 0.0003 & -0.0003 & -0.0005 \\ 0.0049 & -0.0034 & 0.0017 & 0.0017 & -0.0034 \\ 0 & 0.0027 & -0.0044 & 0.0044 & -0.0027 \\ -0.0061 & -0.0019 & 0.0050 & 0.0050 & -0.0019 \end{bmatrix}$$

In simulation, by comparing the true system eigenvalues with reconstructed (with or without noises), the proposed closed-loop algorithm will be tested. The analytical model which was discussed in chapter 3 is used as true model here. First, from the system and controller state-space parameters given, 5000 points of output data are generated in time domain by applying random input data with or without processing and measurements noises. An example of input and output data is shown in Figure 5.3. The next step is to convert time data into frequency data via FFT (Fast Fourier Transformation). Then FRFs are calculated from input and output data in the frequency domain. In the simulation, one may have 30 FRFs because there are five inputs and 6 outputs. The FRF of the first input and output is shown for a 2% noise case in Figure 5.4. Table 5.1 compares the reconstructed system eigenvalues (2% noise and 10% noise) with true ones. The identified result shows a perfect match when there is no noise, which is not shown, and quite good agreement even when there is 2% or 10% of processing and measurement noise. After the closed-loop identification is performed, the open-loop Markov parameters of the identified model are reconstructed. Figure 5.5 shows the comparison of the (1,1) element of the true and reconstructed system Markov parameters. Also, whether or not one can get the same output with the true case from the identified model will be checked by comparing the outputs from both of the true and identified models when we applied the same inputs, shown in Figure 5.6.

Two experiments are also performed for closed-loop identification with a known dynamic output feedback controller which is shown in the Appendix. A total of 8192 data

points at a sampling rate of 250 Hz from each sensor are used for identification. In this experiment, five tests were run and each had white noise on a single actuator, and zero input to the other actuators. In other words, only one row of each of (5×8192) input data has a non-zero value. Finally, five sets of (5×8192) input data and five sets of (6×8192) output data are collected for frequency response function. It is worthy noting that only the first half of input have excitation value and the second half will be zeros for FFT. The reason is FFT is mathematically derived for infinite number of time data whereas the only finite number of time data are available in the real world. To use the finite number of time data, the input-output data should be periodic so that one cycle of data can be used for FFT instead of infinite number. To make the system behave periodic, the zero input is necessary to drive the system to the zero point. FRFs are calculated after time domain data are converted to frequency domain via FFT same as in the simulation. Thirty FRFs from five inputs and six outputs are simultaneously used to identify a state-space system model. The order of the matrix polynomial is set to 13, which is proved to be large enough in chapter 4, and the system order for ERA is set to 70. The reason to choose 70 as the system order for ERA is there is sharp decrease in singular value plot as you can see in Figure 5.7. The identified eigenvalues from testing are shown in Table 5.2.

Numerical simulation is also performed for uncertainty model identification. Two models are identified for 10- and 12- states from the same test data to generate new output data by applying random input without noise. The maximum singular value of differences in FRFs between the two models for each frequency are regarded as a parameter of the uncertainty model without noise. Then ten sets of input-output, five for 10-state model and five for 12-state model, are generated by applying random input with 1% processing and measurement noise. The corresponding ten FRF data are obtained and the averaged FRF is used for closed-loop identification and the identified state-space model is treated as the nominal model. For each frequency, the normalized differencies between averaged FRF and

ten FRFs are calculated and their corresponding maximum singular values are computed. After collecting the largest singular value for each frequency out of 10 cases, the worst case out of ten uncertainty models is constructed. In figure 5.8, two identified models from test data, one for 10-state and the other for 12-state, are compared. Here it should be pointed out that 10-state model can be regarded as a source of the unstructured uncertainty because the 12-state model shows a better agreement with the real test data. The maximum singular value plots for the 10-state model, 12-state model and the identified nominal model of ten noise cases are shown in Figure 5.9. As clearly shown in Figure 5.9, the most differences between 10-state and 12-state models occur at about 400 time steps which is equivalent to around 20 Hz. In Figure 5.10, the maximum singular values of uncertainty models in case of noise free and 1% noise (which is the collection of the worst out of ten noise cases) are shown. The worst singular value of 10 noise cases is about 7 times higher than the worst one of the noise free case.

5.5 Concluding Remarks

A method of identifying an open-loop state-space model from closed-loop input-output frequency response data is developed. The main contribution is that relationship between the open-loop system Markov parameters and the closed-loop FRF is derived for a linear stochastic system with known feedback dynamics. It can also estimate the Kalman filter gain directly without estimating noise covariances. It is also shown that the closed-loop Kalman filter Markov parameters can be calculated through the transfer function matrix between reference input and output data. By identifying the open-loop system successfully from closed-loop input output data in frequency domain, it can be concluded that the recursive closed-loop identification method in time domain which is recently developed, can also be applied to data in the frequency domain. It is shown that the underestimated states

model can cause a serious amount of unstructured uncertainty in identification and can be used to generate the unstructured uncertainty in the numerical simulation. The other hand, process and measurement noise could cause a serious problem when the maximum singular values are used to compare an uncertainty effects to the system. It is also observed that the process and measurement noise doesn't make a big impact to identification itself. By using of the underestimated mode, a simulation model of the uncertainty applying to a future test to design a robust controller is proposed. The proposed model should be tested through experiment to examine the effects of the unstructured uncertainty and the noise in the future.

Table 5.1. Comparison of eigenvalues of analytical and identified model

Analytical Model	Identified from simulation (2 % noise)	Identified from simulation (10 % noise)
1.2651, 1.2601	1.2654, 1.2601	1.2729, 1.2522
1.0399, 0.9616	1.0311, 0.9889	1.0247± j.0427
1.0000± j.0038	1.0088± j.0319	1.0090± j.0659
0.9995± j.0319	1.0048± j.0498	1.0044± j.0453
0.7936, 0.7905	0.7931, 0.7900	0.7987± j.0028

Table 5.2. Comparison of eigenvalues of analytical and identified model

Analytical Model	Identified from Testing (I)	Identified from Testing (II)
1.2651, 1.2601	1.2905, 1.2779	1.2892, 1.2796
1.0399, 0.9616	1.0123± j.0397	1.0280, 0.8233
1.0000± j.0038	0.9885± j.0519	1.0138±.0232i
0.9995± j.0319	0.9894± j.0163	0.9914±.0302i
0.7936, 0.7905	0.7981, 0.7828	0.8828, 0.7772

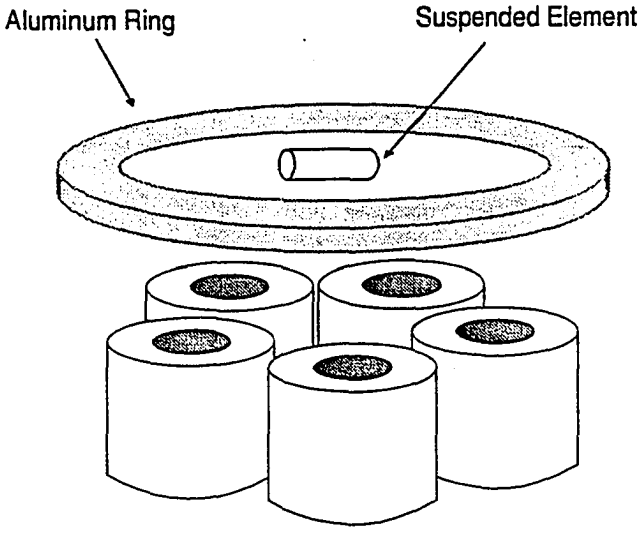

Figure 5.2 Perturbed LAMSTF system with aluminum ring to provide eddy currents

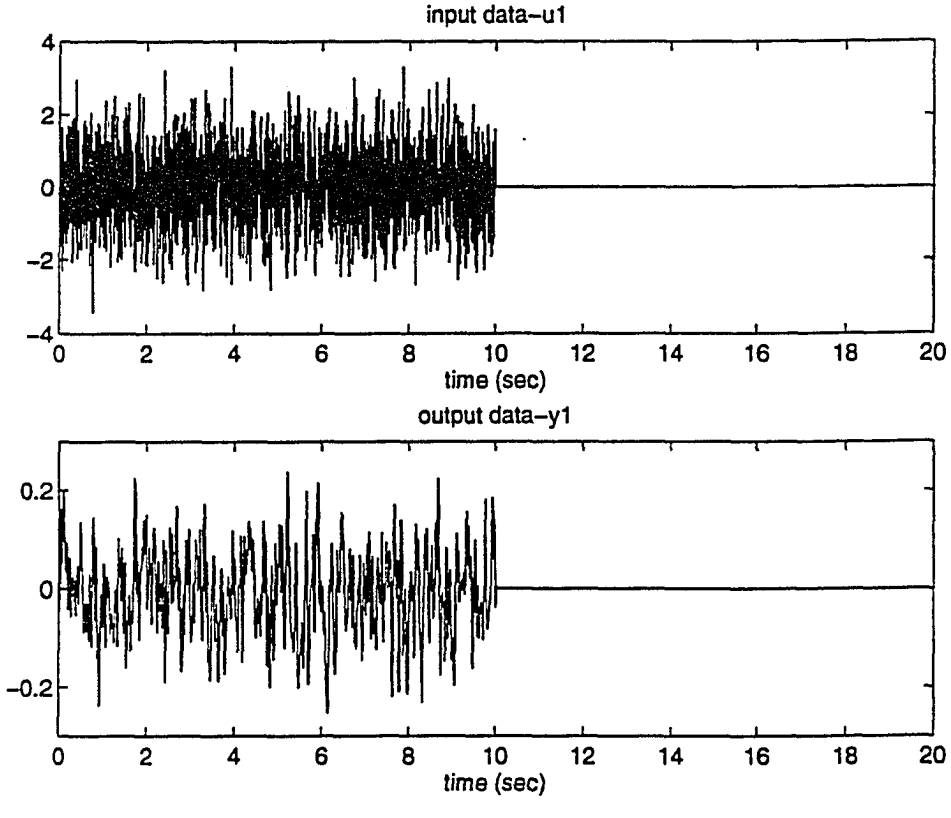

Figure 5.3 Example of input and output data for simulation

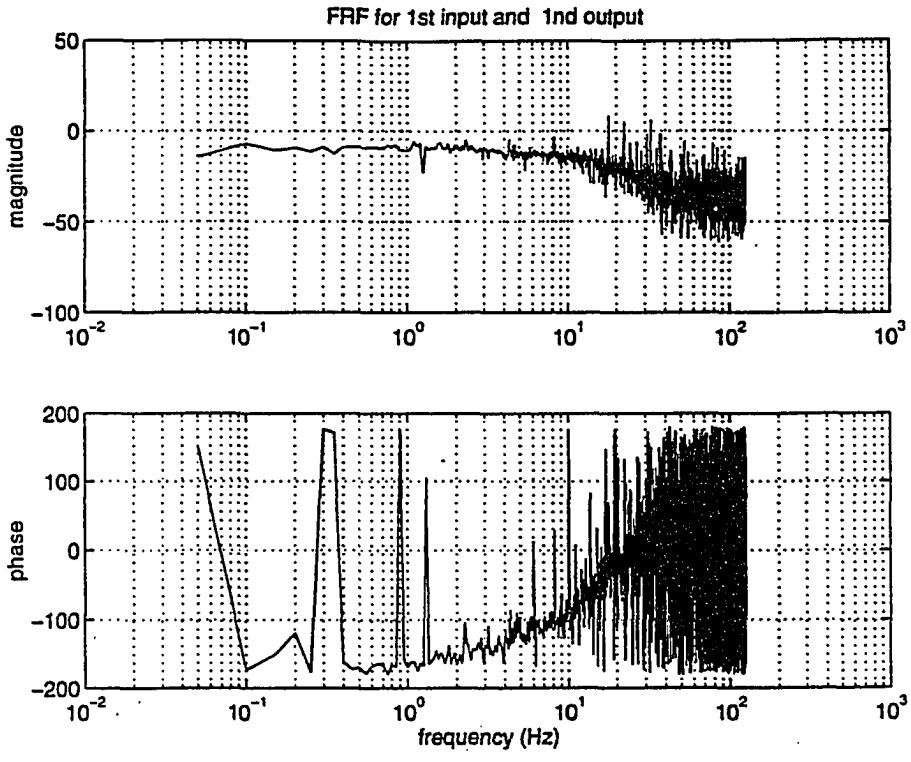

Figure 5.4 Open-loop FRF for the first input and output (2% noise)

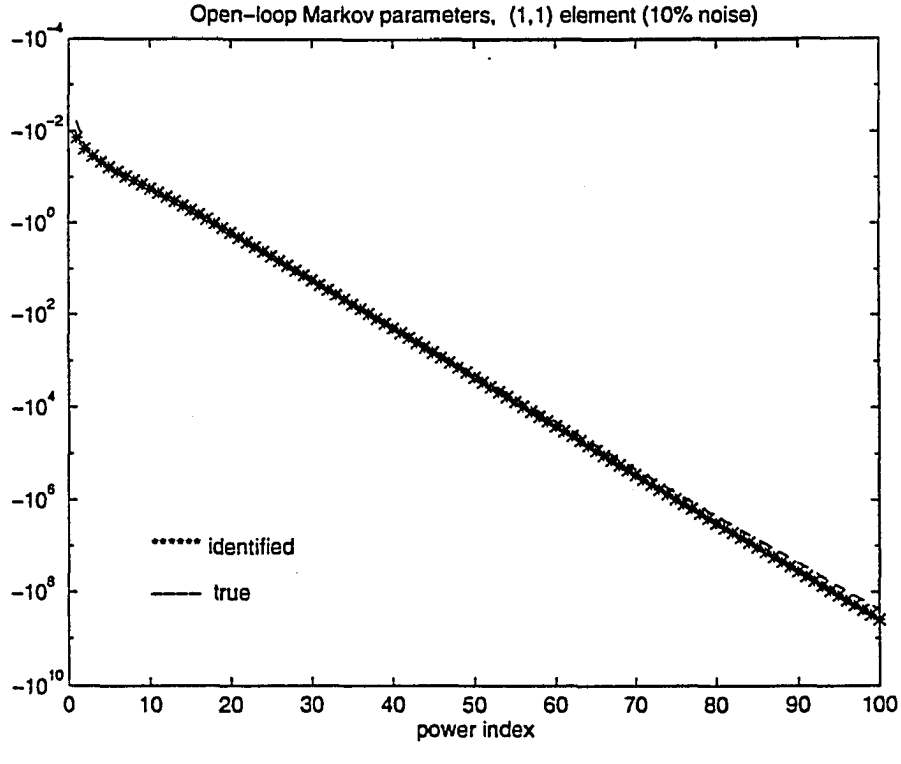

Figure 5.5 Comparison of (1,1) element of true and reconstructed Markov parameters

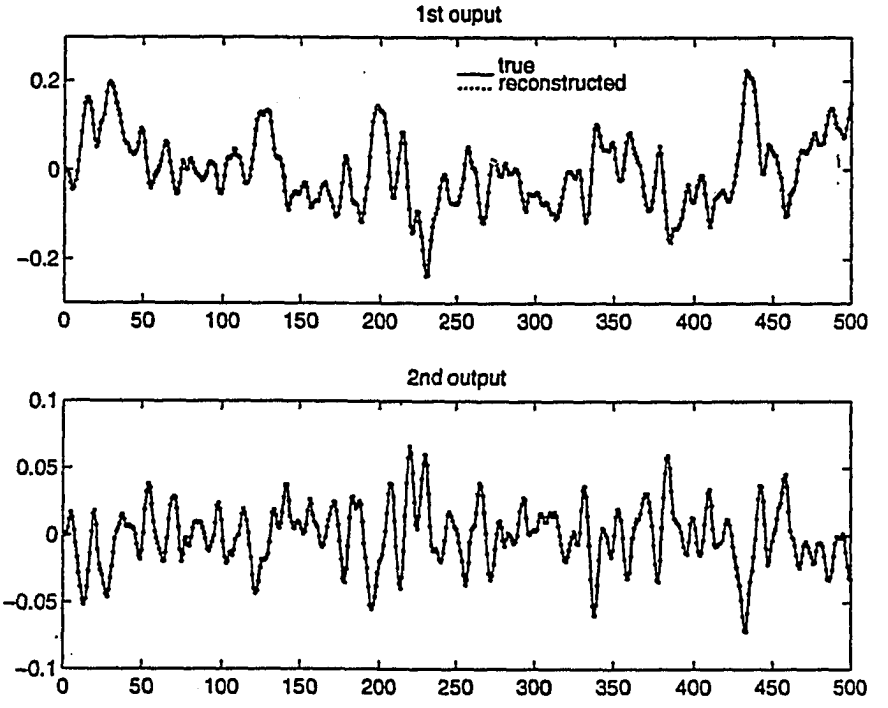

Figure 5.6 Comparison of the output between true and reconstructed model

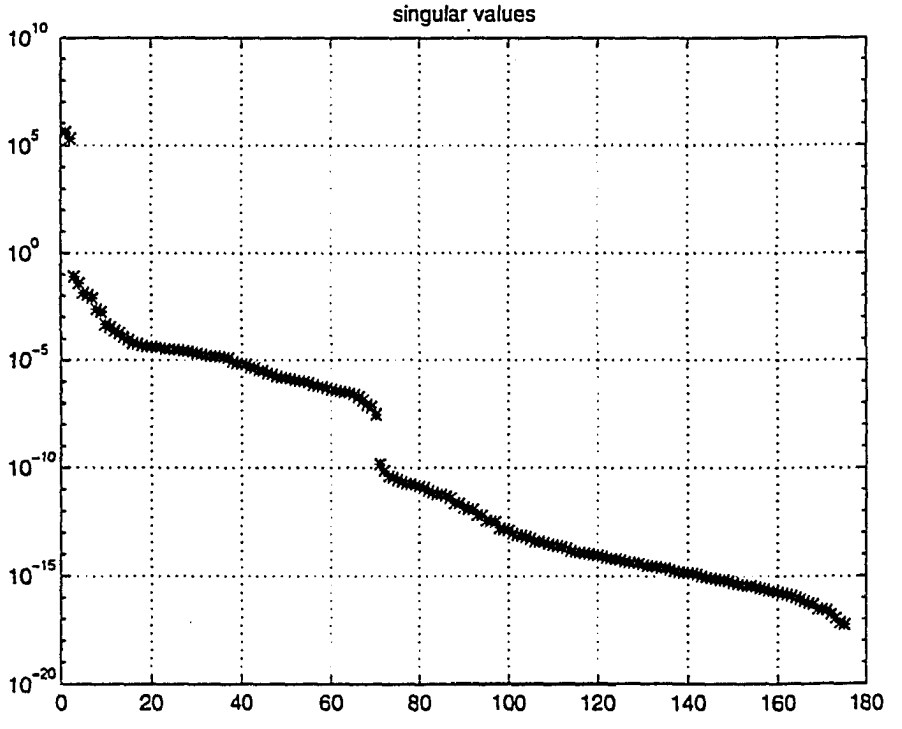

Figure 5.7 Singular Value Plot

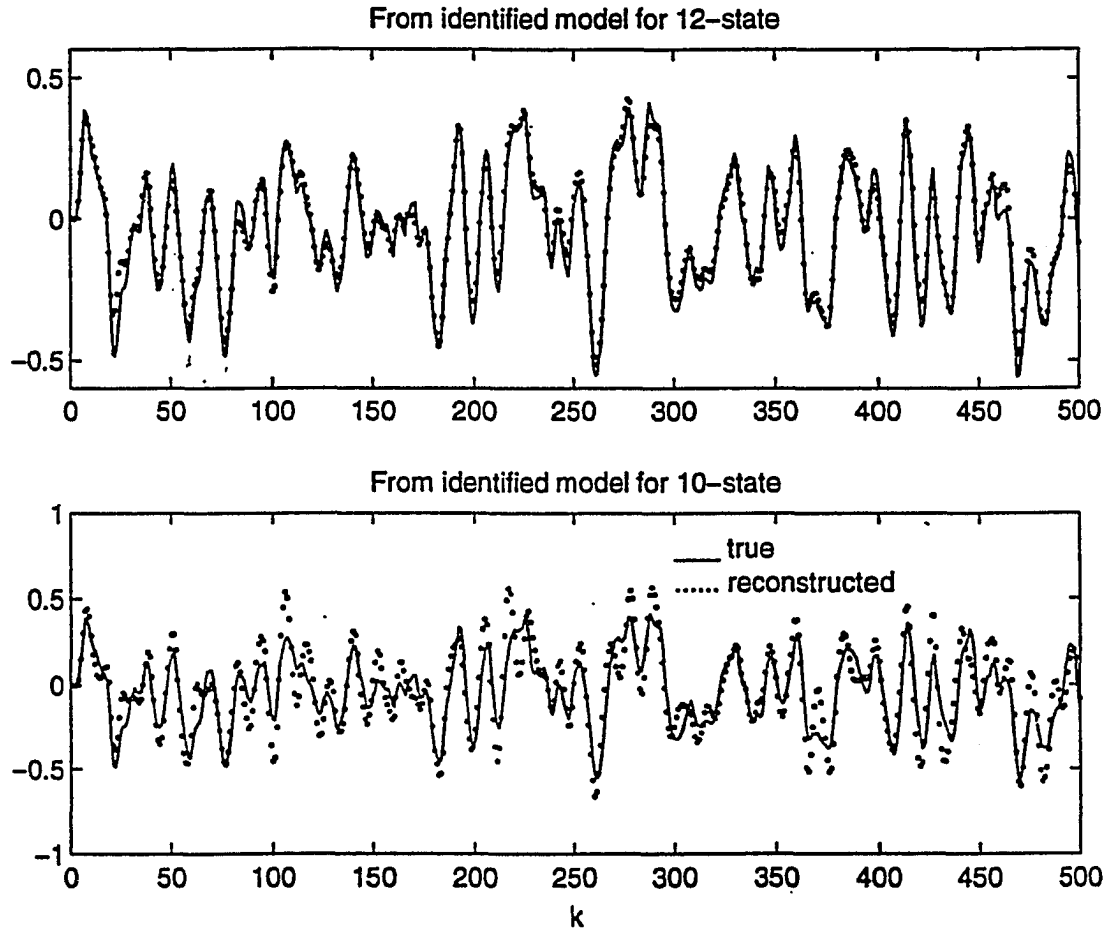

Figure 5.8 Comparison of the output between true and reconstructed model

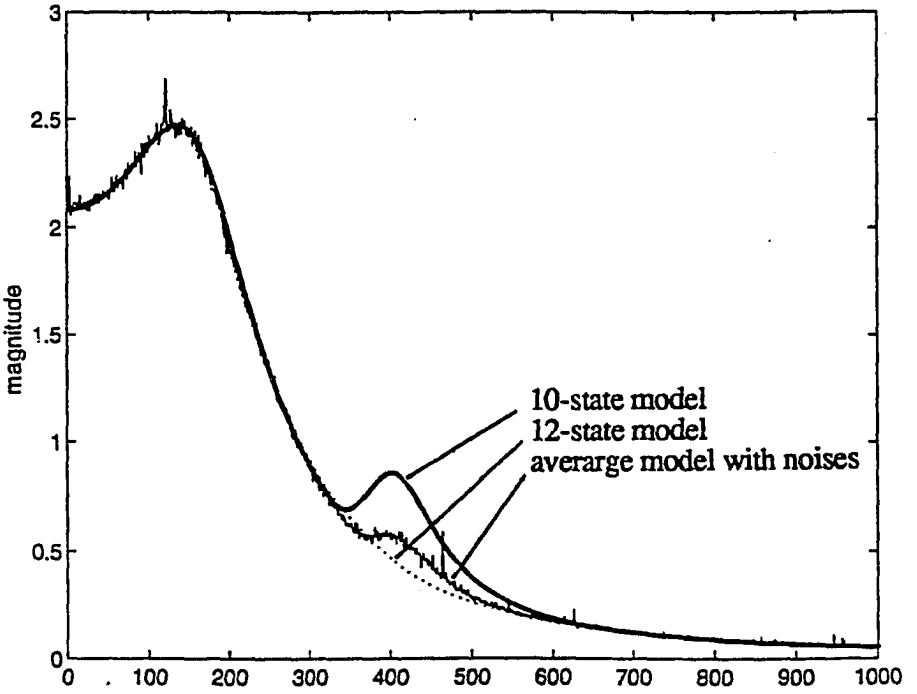

Figure 5.9 Comparison of the max. singular values of closed-loop FRF

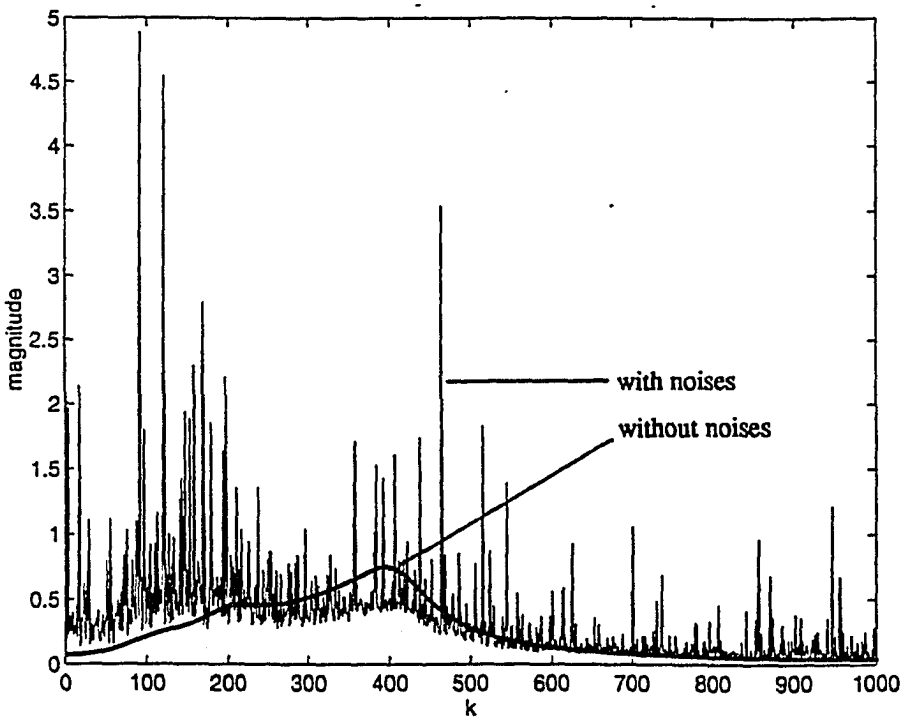

Figure 5.10 Comparison of the max. singular values of closed-loop uncertainty FRF

Chapter 6

CONCLUSIONS

6.1 Contributions

Closed-loop identification methods have been proposed for linear stochastic system. In time domain, projection filter is presented to identify system of unknown feedback dynamics. In frequency domain, the relation between closed-loop system parameters and Frequency Response Function is presented to identify open-loop system from closed-loop input-output data and the simulation model of uncertainty has been proposed to be used for robust controller design.

In the existing closed-loop system identification methods, the Kalman filter has been used to handle noises in process and measurement. But the Kalman filter requires a priori knowledge of covariances of process and measurement noises which are either only partially known or totally unknown. Another limitation is that it can neither adjust itself to trace a changing environment, nor can it correct the error caused by incorrect a priori information. Moreover, after reaching its steady state, the filter "sleeps". That is, no matter

how big the estimation error could be due to whatever reasons, the filter just remains unchanged. In this dissertation, a closed-loop identification method using projection filter is derived, which can simultaneously identify an open-loop system, controller gain and Kalman filter gain by using closed-loop input-output data without knowledge of covariances of process and measurement noises. Also most of closed-loop identification methods require knowledge of feedback dynamics to identify the open-loop system and Kalman filter gain. But in this dissertation the recursive relation between the open-loop Markov parameters and the coefficients of ARX has been derived to identify the open-loop system, Kalman filter gain and controller gain without information of feedback dynamics.

With the advent of sophisticated spectrum analyzers and associated automatic test equipment and also with many failures of LQG controller in real environment which has been dominant player of modern optimal control theory, many researchers begin to pay attention back to frequency domain analysis. Too much emphasis on optimality, and not enough attention to the model uncertainty issue have been accused of the main culprit. In the dissertation, a relation between closed-loop system parameters and FRF has been derived to identify the open-loop system parameter and Kalman filter gain from input-output data in frequency domain . After getting FRF from reference input and system output, the closed-loop system and Kalman filter Markov parameters can be recursively calculated from the estimated matrix polynomials of FRF. Then the open-loop system and Kalman filter Markov can be derived from the closed-loop Markov parameters, finally to be used to identify the open-loop system and Kalman filter gains. Then it is shown that the underestimated states model can cause a serious amount of unstructured uncertainty in identification. Also it is shown that the process and measurement noise can worse a situation when the maximum singular value is used to quantify an uncertainty existing in the system, even though the noise don't make a major difference in identification results. A

simulation model of uncertainty is proposed to study robust controller design by introducing the underestimated state modes and the process and measurement noises.

6.2 Further Extension of the Research

The algorithms developed in this dissertation can be applied or extended further to other areas. For the time domain closed-loop identification, a systematic explanation should be explored how the optimal ARX number can be found without trial and error process and why it should be the particular number. It will make the method more efficient numerically to be used for adaptive or iterative controller design. Also we need to extend the algorithm to when we don't have full state information, which is a more practical case.

For the frequency domain method, the proposed maximum singular value of uncertainty model should be examined in test process how efficiently it can be used to robust controller design. Up until recently, the robust control community has largely taken for granted certain types of uncertainty description, e.g., parameters lying in fixed intervals or H_∞ frequency domains, without questioning how these descriptions might be obtained in practice. More systematic approach should be addressed to enable robust high-performance feedback design of systems which would be otherwise difficult to characterize and control reliably. The systematic approach to come in the future should be an integrated method for system identification, modeling, and robust control.

REFERENCES

1. Chen, C. W., Huang, J.-K., Phan, M., and Juang, J.-N, "Integrated System Identification and Modal State Estimation for Control of Flexible Space Structures." *Journal of Guidance, Control and Dynamics*, Vol. 15, No. 1, 1992, pp. 88-95.

2. Phan, M., Juang, J.-N., and Longman, R. W., "Identification of Linear Multivariable Systems from a Single Set of Data by Identification of Observers with Assigned Real Eigenvalues," *Journal of Astronautical Sciences*, Vol. 40, No. 2, 1992,, pp. 261-279.

3. Phan, M,, Horta, L. G., Juang, J.-N., and Longman, R. W., "Linear System Identification via an Asymptotically Stable Observer", *Proceedings of the AIAA Guidance, Navigation and Control Conference*, New Orleans, LA, Aug. 12-14, 1991, pp. 1180-1194, Also to appear in *Journal of Optimization and Application.*

4. Juang, J.-N., Phan, M., Horta, L. G. and Longman, R. W., "Identification of Observer/Kalman Filter Markov Parameters: Theory and Experiments," *Journal of Guidance, Control , and Dynamics*, Vol. 16, No. 2, March-April 1993, pp. 320-329.

5. Phan, M., Horta, L. G., Juang, J.-N., and Longman, R. W., "Improvement of Observer/Kalman Filter Identification by Residual Whitening," *Proceedings of Eight VPI & SU Symposium*, edited by L. Meirovitch, Blacksburg, Virginia, May, 1991, pp. 467-478.

6. Chen, C. W., Huang, J.-K., and Juang, J.-N., "Identification of Linear Stochastic Systems Through Projection Filters," *Proceedings of the AIAA Structures, Structural Dynamics and Materials Conference*, Dallas, TX, 1992, pp. 2330-2340. .

7. Chen, C. W., Lee, G., and Juang, J.-N., "Several Recursive Techniques for Observer/Kalman Filter System Identification From Data," Paper No. 92-4386, *Proceedings of AIAA Guidance, Navigation and Control Conference*, Hilton Head, SC, August, 1992.

8. Juang, J.-N., and Phan, M., "Linear System Identification via Backward Observer Models," *NASA Technical Memorandum TM-107632*, May 1992.

9. Huang, J.-K., Juang, J.-N. and Chen, C. W., "Single-Mode Projection Filters for Modal Parameter Identification for Flexible Structures," *AIAA Journal of Guidance, Control and Dynamics*, Vol. 12, No. 4, July-August 1989, pp. 568-576.

10. Chen, C. W., Juang, J.-N., and Huang, J.-K., "Adaptive Linear System Identification and State Estimation." in *Control and Dynamic Systems: Advances in Theory and Applications, Vol. 57, Multidisciplinary Engineering Systems: Design and Optimization Techniques and Their Application*, edited by C. T. Leondes. New York: Academic Press, Inc., 1993, pp. 331-368.

11. Juang, J.-N., Phan, M., "Identification of System, Observer, and Controller from Closed-Loop Experimental Data," *Journal of Guidance, Control, and Dynamics*, Vol. 17, No. 1, 1994, pp. 91-96.

12. Hu, A., and Martin, D., "System Identification of Unstable Manipulators Using ERA Methods," *Proceedings. of the AIAA Guidance, Navigation and Control Conference*, 1993, pp. 1264-1270.

13. Phan, M., Juang, J.-N., Horta, L. G., and Longman, R. W., "System Identification from Closed-Loop Data with Known Output Feedback Dynamics," NASA TM-107604, April, 1992, also to appear in *AIAA Journal of Guidance, Control and Dynamics*.

14. Liu, K., and Skelton, R. E., "Closed-Loop Identification and Iterative Controller Design," *Proceedings of the IEEE Design and Control Conference*, Honolulu, Hawaii, Dec. 1990, pp. 482-487.

15. Doyle, B. A. and Stein, G., "Robustness with Observers," *IEEE Trans. Automatic Control*, Vol. 24, 1979, pp. 607-611.

16. Bayard, D. S., "An Algorithm for State Space Frequency Domain Identification without Windowing Distortions,", *Proceedings of the Control and Design Conference*, 1992.

17. Juang, J.-N. and Pappa, R. S., "An Eigensystem Realization Algorithm for Modal Parameter Identification and Modal Reduction," *Journal of Guidance, Control, and Dynamics*, Vol. 8, No. 5, 1985, pp. 620-627.

18. Juang, J.-N., Cooper, J. E., and Wright, J. R., "An Eigensystem Realization Algorithm Using Data Correlations (ERA/DC) for Modal Parameter Identification," *Control Theory and Advanced Technology*, Vol. 4, No. 1, 1988, pp. 5-14.

19. Chen, C-W, Juang, J-N. and Lee, G., "Frequency Domain State-Space System Identification," NASA TM-107659, June 1992.

20. Kosut, R. L., Goodwin, G. C., and Polis, M. P., *Special Issue on System Identification for Robust Control Design, IEEE Trans. on Automatic Control*, Vol. 37, No. 7, 1992.

21. Ljung, L., *System Identification-Theory for the User*, Prentice-Hall, Inc., Englewood Cliffs, New Jersey, 1987.

22. Shen, J. Y., Huang, J.-K., and Taylor, Jr., L. W., "Likelihood Estimation for Distributed Parameter Models of Large Beam-Like Structures," *Journal of Sound and Vibration*, Vol. 155, No. 3, 1992, pp. 467-480.

23. Shen, J. Y., Huang, J.-K., and Taylor, Jr. L. W., "Timoshenko Beam Modeling for Parameter Estimation of NASA Mini-Mast Truss," *ASME Journal of Vibration and Acoustics*, Vol. 115, No. 1, January 1993, pp. 19-24.

24. Huang, J.-K., Hsiao, M.-H. and Cox, D. E., "Identification of Linear Stochastic Systems from Closed-Loop Data with Known Feedback Dynamics," *Proceedings of AIAA Structures, Dynamics and Materials Conference*, Hilton Head, SC, April 1994, pp. 1619-1627,

25. Chen, C. T., *Linear System Theory and Design*, Second Edition, Chapter 6, CBS College Publishing, New York, 1984.

26. Haykin, S., Adaptive Filter Theory, Second edition, Prentice-Hall Inc. Englewood Cliffs, New Jersey. 07632, 1991.

27. Goodwin, G. C., and Sin K. S., *Adaptive Filtering, Prediction and Control*, Prentice-Hall, Englewood Cliffs, New Jersey 07632, 1984.

28. Groom, N. J., Britcher, C. P., "A Description of a Laboratory Model Magnetic Suspension Test Fixture with Large Angular Capability," *Proc. of the IEEE Conference on Control Applications*, Vol. 1, pp. 454, 1992.

29. Ghofrani, M., "Approaches to Control of the Large Angle Magnetic Suspension Test Fixture," Master Thesis, Old Dominion University, Dec. 1992, and NASA CR-191890, Dec. 1992.

30. Groom, N. J., "Analytical Model of a Five Degree of Freedom Magnetic Suspension Systems using Electromagnets Mounted in a Planar Array," NASA CP-10066, Vol. 1, March 1991, pp. 355-376.

31. Groom, N. J., Britcher, C. P., "Open-Loop Characteristics of Magnetic Suspension Systems Using Electromagnets Mounted in a Planar Array," *NASA TP* 3229, 1992.

32. Schlee, F.H., Standish, C. J., and Toda, N. F., "Divergence in the Kalman Filter," *AIAA Journal*, Vol. 5, June 1976, pp. 1114-1120.

33. Fitzgerald, "Divergence of the Kalman Filter," *IEEE Trans. Automatic Control*, Dec. 1971.

34. Sangsuk-Iam and Bullock, T. E., "Analysis of Continuous-Time Kalman Filter Under Incorrect Noise Covariances," *Automatica,* Vol. 24, No. 5, 1988, 659-669.

35. Sangsuk-Iam and Bullock, T. E., " Behavior of the Discrete-Time Kalman Filter Under Incorrect Noise Covariances," *Proc. 26th IEEE Conf. on Decision and Control*, Los Angels, California.

36. Chen, C.-W., "Integrated System Identification and Adaptive State Estimation for Control of Flexible Space Structures," Ph.D. Dissertation, Old Dominion University, August, 1991.

37. Elbert, T. F., *Estimation and Control of System*, New York: Van Nostrand Reinhold Co.1984.

38. Larimore, W. E., Mehra, R. K., "The Problem of Overfitting Data," *Byte 10*, 1985, pp. 167-180.

39. Oppenheim, A. V. and Schafer, R. W., *Digital Signal Processing*, Prentice-Hall Inc. Englewood Cliffs, New Jersey., 1975.

40. Lim, K. B., and Cox, D. E., "Experimental Robust Control Studies on an Unstable Magnetic Suspension System," *American Control Conference*, Baltimore, MD., 1994.

41. Lim, K. B., and Cox, D. E. "Robust Tracking Control of a Magnetically Suspended Rigid Body," *Submitted for publication*, 1994.

42. Cox, D. E., and Groom, N. J., Hsiao, M.-H., Huang, J.-K., "Identification of a Large-Angle Magnetic Suspension System," *Submitted for publication in Journal of Sound and Vibration*, 1995.

APPENDIX A

A finite-dimensional, linear, discrete-time, time-invariant system can be modeled as:

$$x_{k+1} = Ax_k + Bu_k + w_k \tag{A.1}$$

$$y_k = Cx_k + v_k. \tag{A.2}$$

Here, the state-space parameters of LAMSTF are shown for a sampling rate of 250 Hz as follows:

$A = [A_{11} \quad A_{12}]$

$$A_{11} = \begin{bmatrix} 1.1687 & 0.0006 & -0.0000 & 0.0000 & 0.0000 \\ -0.0000 & 1.1629 & -0.0000 & -0.0000 & -0.0000 \\ -0.0000 & 0.0001 & 1.0178 & -0.0017 & -0.0037 \\ -0.0000 & 0.0000 & 0.0001 & 1.0051 & 0.0001 \\ 0.0000 & 0.0002 & -0.0004 & 0.0008 & 1.0106 \\ 0.0000 & -0.0000 & -0.0021 & -0.0240 & 0.0005 \\ 0.0000 & -0.0001 & -0.0064 & -0.0001 & -0.0213 \\ -0.0000 & -0.0000 & 0.0109 & -0.0009 & -0.0045 \\ 0.0000 & -0.0000 & -0.0086 & 0.0009 & 0.0032 \\ 0.0000 & -0.0000 & 0.0004 & 0.0002 & 0.0006 \end{bmatrix}$$

$$A_{12}=\begin{bmatrix} 0.0000 & 0.0000 & -0.0000 & -0.0000 & -0.0000 \\ -0.0000 & 0.0000 & -0.0000 & 0.0000 & -0.0000 \\ 0.0021 & 0.0074 & -0.0127 & 0.0112 & 0.0006 \\ 0.0295 & 0.0006 & 0.0015 & -0.0011 & 0.0003 \\ -0.0018 & 0.0223 & 0.0066 & -0.0039 & 0.0030 \\ 0.9908 & 0.0028 & -0.0010 & 0.0003 & -0.0011 \\ -0.0041 & 0.9692 & 0.0064 & 0.0004 & 0.0003 \\ 0.0021 & 0.0050 & 0.9260 & -0.0549 & 0.0028 \\ 0.0009 & 0.0031 & -0.0589 & 0.9125 & -0.0008 \\ 0.0012 & 0.0545 & -0.0002 & -0.0002 & 0.8652 \end{bmatrix}$$

$$B=\begin{bmatrix} 0.0035 & 0.0706 & 0.0519 & -0.0363 & -0.0633 \\ -0.0434 & -0.0326 & -0.0340 & -0.0425 & -0.0396 \\ 0.0580 & -0.0454 & 0.0983 & -0.0361 & 0.0254 \\ -0.0926 & -0.0315 & 0.0881 & 0.0865 & -0.0218 \\ 0.1160 & 0.0124 & 0.0263 & 0.0982 & -0.0242 \\ -0.1015 & -0.0368 & 0.1033 & 0.0854 & -0.0154 \\ 0.1373 & 0.0057 & 0.0719 & 0.0859 & -0.0066 \\ -0.0159 & -0.0637 & -0.1326 & 0.1165 & 0.0625 \\ 0.0158 & -0.1531 & -0.0261 & 0.0041 & 0.1245 \\ -0.0484 & -0.0800 & -0.0513 & -0.0553 & -0.1009 \end{bmatrix}$$

$$C=[C_{11} \quad C_{12}]$$

$$C_{11}=\begin{bmatrix} -0.0313 & 0.4029 & -0.0469 & 0.2269 & -0.0381 \\ 0.0291 & -0.4213 & 0.0006 & 0.2248 & 0.0290 \\ -0.4423 & 0.1071 & 0.1809 & 0.0553 & 0.0669 \\ -0.4254 & -0.1184 & -0.1787 & -0.0092 & -0.0829 \\ 0.4495 & -0.0763 & 0.0574 & 0.0273 & -0.1861 \\ 0.3889 & 0.1015 & -0.0614 & 0.0085 & 0.1739 \end{bmatrix}$$

$$C_{12}=\begin{bmatrix} -0.1961 & 0.1274 & -0.0363 & 0.0198 & -0.1513 \\ -0.2097 & -0.1079 & -0.0130 & 0.0297 & 0.1502 \\ -0.0618 & -0.0906 & -0.0418 & -0.2228 & -0.0472 \\ 0.0200 & 0.1217 & -0.2197 & -0.0559 & 0.0630 \\ -0.0400 & 0.1239 & 0.2109 & 0.0827 & 0.0464 \\ 0.0012 & -0.1277 & 0.0386 & 0.1913 & -0.0634 \end{bmatrix}$$

For simulation, the discrete-time state-space parameters of dynamic output feedback controller can be modeled as:

$$p_{k+1} = A_d p_k + B_d y_k \tag{A.3}$$

$$u_k = C_d p_k + D_d y_k + r_k, \tag{A.4}$$

The matrices are

$$A_d = \begin{bmatrix} 0.3333 & 0 & 0 & 0 & 0 \\ 0 & 0.3333 & 0 & 0 & 0 \\ 0 & 0 & 0.6000 & 0 & 0 \\ 0 & 0 & 0 & 0.6000 & 0 \\ 0 & 0 & 0 & 0 & 0.6000 \end{bmatrix}$$

$$B_d = \begin{bmatrix} -0.0206 & 0.0206 & 0 & 0 & 0 & 0 \\ 0 & 0 & -0.0098 & -0.0098 & 0.0098 & 0.0098 \\ 0 & 0 & 0.0003 & -0.0003 & -0.0003 & 0.0003 \\ 0 & 0 & -0.0003 & 0.0003 & -0.0003 & 0.0003 \\ 0.0004 & 0.0004 & 0 & 0 & 0 & 0 \end{bmatrix}$$

$$C_d = 1.0e+03 * \begin{bmatrix} 0.0796 & 0.0000 & 7.3872 & 0.0000 & -5.5493 \\ 0.1032 & 0.0716 & -5.9772 & 4.3222 & -1.7160 \\ 0.0886 & 0.0442 & 2.2836 & -6.9917 & 4.4907 \\ 0.0886 & -0.0442 & 2.2836 & 6.9917 & 4.4907 \\ 0.1032 & -0.0716 & -5.9772 & -4.3222 & -1.7160 \end{bmatrix}$$

$$D_d = \begin{bmatrix} 10.8171 & 3.9903 & -7.0133 & 7.0133 & 7.0133 & -7.0133 \\ 6.7151 & -2.1362 & 11.2687 & -8.3349 & -3.0144 & 0.0807 \\ -2.1923 & -9.7904 & -7.9381 & 9.7505 & -5.4144 & 3.6020 \\ -2.1923 & -9.7904 & 3.6020 & -5.4144 & 9.7505 & -7.9381 \\ 6.7151 & -2.1362 & 0.0807 & -3.0144 & -8.3349 & 11.2687 \end{bmatrix}$$

For experiments, the discrete-time state-space parameters of dynamic output feedback controller of (A.3) and (A.4) are listed as follows:

$$A_d = \begin{bmatrix} 0.1111 & 0 & 0 & 0 & 0 \\ 0 & 0.1111 & 0 & 0 & 0 \\ 0 & 0 & 0.4286 & 0 & 0 \\ 0 & 0 & 0 & 0.4286 & 0 \\ 0 & 0 & 0 & 0 & 0.4286 \end{bmatrix}$$

$$B_d = 1.0e+05 * \begin{bmatrix} -0.0000 & 0.0000 & -0.0000 & -0.0000 & 0.0000 & 0.0000 \\ -0.0003 & 0.0003 & 0.0000 & 0.0000 & -0.0000 & -0.0000 \\ -0.9021 & -0.9021 & -1.4372 & 1.4372 & -1.4378 & 1.4378 \\ -0.9018 & -0.9018 & -1.4373 & 1.4373 & -1.4379 & 1.4379 \\ -0.0000 & -0.0000 & -0.0002 & 0.0002 & 0.0002 & -0.0002 \end{bmatrix}$$

$$C_d = \begin{bmatrix} 0.0000 & 0.0628 & 0.0940 & -0.0940 & -0.1220 \\ 0.0613 & 0.0814 & -0.0033 & 0.0033 & 0.0988 \\ 0.0379 & 0.0699 & -0.0236 & 0.0236 & -0.0378 \\ -0.0379 & 0.0699 & -0.1289 & 0.1289 & -0.0378 \\ -0.0613 & 0.0814 & 0.0618 & -0.0618 & 0.0988 \end{bmatrix}$$

$$D_d = \begin{bmatrix} 9.7516 & 3.7430 & -6.3953 & 6.3953 & 6.3953 & -6.3953 \\ 5.9817 & -1.8087 & 10.2313 & -7.6492 & -2.7002 & 0.1180 \\ -2.1164 & -8.8038 & -7.2708 & 8.8660 & -4.9120 & 3.3168 \\ -2.1164 & -8.8038 & 3.3168 & -4.9120 & 8.8660 & -7.2708 \\ 5.9817 & -1.8087 & 0.1180 & -2.7002 & -7.6492 & 10.2313 \end{bmatrix}$$

APPENDIX B

```
function [G,yf,uf]=frf(ys,us);
% convert time data to frequency data via fft
%
%
  [noi,N]=size(ys);
  [ni,N]=size(us);
  no=noi/ni;
  no1=no-1;
  n1=0;
%
  yf=fft(ys')';
  uf=fft(us')';
%
  nd=fix(N/2);
  G=zeros(no,nd*ni);
for i=2:nd+1
    k1=0;
  for k=1:ni
    k1=k1+1;
    k2=k1+no1;
    n1=n1+1;
    G(:,n1)=yf(k1:k2,i)/uf(k,i);
    k1=k2;
  end;
end;
%
%
%
%
%
function [Ai,Bi,Ci,Di,Ki,mo,Y,no,q]=clidf(G,a,b,c,d,TS)
% G= Frequency Response Function;
% TS= spampling time;
% output data y(no,N);
% no=number of outputs
% input data r(ni,N);
% ni=number of inputs
% N=number of data points
  [ni,n]=size(c);
  [no,N]=size(G);
  nd=N/ni;
  p=no+ni;
```

```
input('order of ARX mode=(0=skip)');
  if ans~=0,
    q=ans;
    input('identify D(1=yes,0=no)');
    th=arx_fre(G,q,ans,nd,1,0);
                    % coefficient of ARX model;
  end;
input('number of Markov parameters for ERA=(0=skip)');
  if ans~=0
    n=ans;
    Ak=eye(size(a));
    h=zeros(ni,no*(n+1));
    h(:,1:no)=d;
       for i=no:no:n*no,
         h(:,i+1:i+no)=c*Ak*b;
         Ak=a*Ak;
       end;
          no1=no+1;
          ni1=ni-1;
          nom1=no-1;
          nni=np1*ni;
          nno=np1*no;
          Y=zeros(no,nni);
          N=zeros(no,nno);
       for i=1:q+1
         i1=i-1;
         n1=i1*ni+1;
         n2=n1+ni1;
         n3=i1*no+1;
         n4=n3+nom1;
         n11=i1*p+1;
         n12=n11+ni1;
         n21=n11+ni;
         n22=n21+nom1;
         Y(:,n1:n2)=th(1:no,n11:n12);
                    % closed-loop system Markov parameter;
         N(:,n3:n4)=th(1:no,n21:n22);
                    % closed-loop Kalman filter Markov parameter;
       end;
         Y=markov(Y,N,0,n);
         N=markov(N,N,1,n);
         [Y,E]=clmarkov(Y,h,n,N);
                    % open-loop Markov parameter;
  end;
          [Ai,Bi,Ci,Di,H]=era(Y,no,q);
                    % Eigensystem Realization Algorithm;
          Ki=kalman(Ai,Ci,E,n);
                    % Identify Kalman filter gain;
%
%
%
%
%
```

```
function th=arx_fre(G,q,d,nd,fb,fe)
% identify parameters of ARX model using least square in batch
% y(k+1)=sum(a(i)y(k-i))+sum(b(i)u(k-i)),i=0,1,...,q
% q=order of arx model
% y=noxk of output data;
% u=nixk of input data;
% N=number of data points;
% no=nimber of outputs;
% ni=number of inputs
% th=[b(0) a(0) b(1) a(1)... b(q) a(q)]
%
%
  [no,N]=size(G);
  ni=N/nd;
  p=no+ni;
  ni1=ni-1;
  I=eye(ni);
  w=pi/nd*sqrt(-1);
  z=zeros(q,nd);
    for i=1:q;
      for k=1:nd,
        z(i,k)=exp(w*k)^i;
      end;
    end;
if d==1
  phi=zeros(p*q+ni,N);
  n=ni;
      for i=1:nd,
         n1=(i-1)*ni+1;
         phi(1:ni,n1:n1+ni1)=I;
      end;
else
  phi=zeros(p*q,N);
  n=0;
end;
    for k=1:nd
       n1=(k-1)*ni+1;
       n2=n1+ni1;
       nn=n;
    for i=1:q
        np=nn+p;
        phi(nn+1:np,n1:n2)=[I;G(:,n1:n2)]*z(i,k);
        nn=np;
     end;
       n1=n2;
     end;
  n1=fb*ni+1;
  N1=N-fe*ni;
  G=G(:,n1:N1);
  phi=phi(:,n1:N1);
  th=[real(G) imag(G)]/[real(phi) imag(phi)];
  [m,n]=size(th);
if d==1
  th=[th(:,1:ni) zeros(m,no) th(:,ni+1:n)];
else
  th=[zeros(m,p) th];
end;
```

```
function Y=markov(y1,y2,eq,n,y3)
% Y=markov(y1,y2,eq,q,n,no,ni,y3)=y1(k)+
%              sum{y2(i)Y(k-i),1,...,k-eq},k=1,...,n;
%     or if y3 exists,
% Y=y1(k)+sum{y2(i)y3(k-i),1,...,k-eq},k=1,...,n;
% extract Markov parameters from arx model parameters
% Y=nox(nixn) Markov parameters matrix
% no=number of outputs;
% ni=number of inputs
% n=number of Markov parameters
%
%
  [no,ni]=size(y1);
  Y=zeros(no,ni);
  n1=n+1;
  ni=ni/n1;
if exist('y3')==0
  Y(:,1:ni)=y1(:,1:ni);
    for k=1:n
      kk=k*ni;
      h=y1(:,kk+1:kk+ni);
      k1=k-eq;
    for i=1:k1
      ii=i*no;ki=(k-i)*ni;
      h=h+y2(:,ii+1:ii+no)*Y(:,ki+1:ki+ni);
    end;
      Y(:,kk+1:kk+ni)=h;
    end;
else
  [no,ni]=size(y3);ni=ni/n1;
    for k=1:n
      kk=k*ni;
      h=y1(:,kk+1:kk+ni);
      k1=k-eq;
    for i=1:k1
      ii=i*no;
      ki=(k-i)*ni;
      h=h+y2(:,ii+1:ii+no)*y3(:,ki+1:ki+ni);
    end;
      Y(:,kk+1:kk+ni)=h;
    end;
end;
%
%
%
%
function [H,E]=clmarkov(Y,h,n,N)
% Y=markov(y1,y2,eq,q,n,no,ni,y3)=y1(k)
%                 +sum{y2(i)Y(k-i),1,...,k-eq},k=1,...,n;
%       or if y3 exists,
%   Y=y1(k)+sum{y2(i)y3(k-i),1,...,k-eq},k=1,...,n;
% extract Markov parameters from arx model parameters
% Y=nox(nixn) Markov parameters matrix
% no=number of outputs;
% ni=number of inputs
% n=number of Markov parameters
%
```

```
%
  [no,ni]=size(Y);
  n1=n+1;
  ni=ni/n1;H=Y;
  E=zeros(no,no*n1);
  H(:,1:ni)=Y(:,1:ni);
for j=1:n
  jj=j*ni;
  hx=Y(:,jj+1:jj+ni);
  je=j*no;
  ex=N(:,je+1:je+no);
      for k=1:j-1
         jk=(j-k)*ni;
         jke=(j-k)*no;
      for i=1:k
          ii=i*ni;
          ki=(k-i)*no;
      hx=hx-H(:,ii+1:ii+ni)*h(:,ki+1:ki+no)*Y(:,jk+1:jk+ni);
      ex=ex-H(:,ii+1:ii+ni)*h(:,ki+1:ki+no)*N(:,jke+1:jke+no);
      end;
      end;
  H(:,jj+1:jj+ni)=hx;
      for i=1:j
          ii=i*ni;ji=(j-i)*no;
         ex=ex-H(:,ii+1:ii+ni)*h(:,ji+1:ji+no);
      end;
  E(:,je+1:je+no)=ex;
end;
%
%
%
%
%
function K=kalman(A,C,Y,n)
% Calculate Kalman filter gain
% th=[b(0) a(1) b(1) ... a(q) b(q)];
% q=order of ARX model
% n=number of Kalman Markov parameters
% K=Kalman filter gain matrix
% C=output matrix
% A=system matrix
  [no,n2]=size(Y);
  [m,m]=size(A);
  n2no=n2-no;
  O=zeros(n2no,m);
  N=zeros(n2no,no);
  Ak=eye(m);
for i=1:n
  ii=(i-1)*no;
  ii1=ii+1;
  iino=ii+no;
  O(ii1:iino,:)=C*Ak;
  Ak=A*Ak;
  N(ii1:iino,:)=Y(:,iino+1:iino+no);
end;
%
  K=O\N;
%
```

```
function [A,B,C,D,H]=era(H,p,q)
% realize A,B,C,D matrices from markov parameters using ERA
% [A,B,C,D]=era(Y,p,q)
% q=order of ARX model
% Y=mx(pxn) markov parameters matrix
% m=number of outputs;
% p=number of inputs; n=number of Markov parameters
%
%
  Y=H;
  [m,n]=size(Y);
  D=Y(:,1:p);
  Y=Y(:,p+1:n);
  n=n/p-1;
  r=fix(n/(m/p+1));
  s=n-r;
  mr=m*r;
  ps=p*s;
  H1=zeros(mr,ps);
  H2=H1;
for i=1:r
  for j=1:s
    mi=m*(i-1);
    pj=p*(j-1);
    pij=p*(i+j-2);
    H1(mi+1:mi+m,pj+1:pj+p)=Y(:,pij+1:pij+p);
    H2(mi+1:mi+m,pj+1:pj+p)=Y(:,pij+p+1:pij+2*p);
  end;
end;
  [U,S,V]=svd(H1);
  figure(1);
  semilogy(diag(S),'*');%keyboard;
  title(' singular values ');
  grid;
  input('number of states of realized system =');n=ans;
  S=S(1:n,1:n);
  S=sqrt(S);
  SI=inv(S);
  U=U(:,1:n);
  V=V(:,1:n);
  A=SI*U'*H2*V*SI;
  B=S*V'*[eye(p);zeros(ps-p,p)];
  C=[eye(m),zeros(m,mr-m)]*U*S;
%
%
%
%
%
```